

the respective  $^1\text{H}$  NMR resonance shifting from  $\delta$  -6.4 for [4]<sup>-</sup> to  $\delta$  -7.7 for 1 and finally to  $\delta$  -11.9 for  $\text{HFe}_4(\text{CO})_{12}\text{BH}_2$ .<sup>22</sup> (treatment of pure 1 with concentrated HCl generates  $\text{HFe}_4(\text{CO})_{12}\text{BH}_2$  and (2-Me-C<sub>6</sub>H<sub>4</sub>)<sub>3</sub>PAuCl more or less quantitatively).  $[\text{Au}\{\text{P}(2\text{-Me-C}_6\text{H}_4)_3\}_2][4]$  is rapidly and cleanly converted to 1, while complete regeneration of the all-hydrogenated butterfly cluster is a much slower process. There was no attempt to make a detailed kinetic study of the degradation mechanism.

### To Fuse or Not to Fuse?

The reaction of  $[\text{HFe}_4(\text{CO})_{12}\text{BH}]^-$  with 1 equiv of LAuCl leads to the simple monogold derivative  $\text{HFe}_4(\text{CO})_{12}\text{BH-AuL}$ , which is stable with respect to conversion to  $\text{HFe}_4(\text{CO})_{12}\text{BAu}_2\text{L}_2$  only when L is the sterically demanding ligand P(2-Me-C<sub>6</sub>H<sub>4</sub>)<sub>3</sub>. In other cases (L = PMe<sub>3</sub>, PEt<sub>3</sub>, PMe<sub>2</sub>Ph, PMePh<sub>2</sub>) the preferred product is  $[\text{AuL}_2][\{\text{HFe}_4(\text{CO})_{12}\text{BH}\}_2\text{Au}]$ , which, although possessing the same stoichiometry as  $\text{HFe}_4(\text{CO})_{12}\text{BHAuL}$ , contains two  $\{\text{HFe}_4(\text{CO})_{12}\text{BH}\}$  subclusters fused about a gold(I) atom and results from Au-P cleavage and a redistribution of the phosphine ligands. As one goes from  $[\text{HFe}_4(\text{CO})_{12}\text{BH}]^-$  to the ruthenium analog, the tetrametal butterfly increases in size and the reaction of  $[\text{HRu}_4(\text{CO})_{12}\text{BH}]^-$  with LAuCl, even in the case of L = P(2-Me-C<sub>6</sub>H<sub>4</sub>)<sub>3</sub>, leads to the competitive formation of  $\text{HRu}_4(\text{CO})_{12}\text{BHAuP}(2\text{-Me-C}_6\text{H}_4)_3$  and  $\text{Ru}_4(\text{CO})_{12}\text{BHAu}_3\{\text{P}(2\text{-Me-C}_6\text{H}_4)_3\}_2$  as well as  $[\{\text{HRu}_4(\text{CO})_{12}\text{BH}\}_2\text{Au}]^-$ . For the ruthenium clusters, the fused

system  $[\{\text{HRu}_4(\text{CO})_{12}\text{BH}\}_2\text{Au}]^-$  appears to be a particularly favorable product.

**Acknowledgments** are made to the donors of the Petroleum Research Fund, administered by the American Chemical Society, for support of this work, to the SERC for a studentship (to S.M.D.), to the Cambridge Commonwealth Trust and Tate and Lyle Corp. for a studentship (to M.S.S.), and to the NSF for a grant (CHE 9007852) toward the purchase of a diffractometer at the University of Delaware. Johnson-Matthey is thanked for generous loans of RuCl<sub>3</sub>. C.E.H. thanks Dr. Lutz H. Gade for several useful discussions.

**Registry No.** 1, 141292-25-3; 2, 141292-27-5; 3 (isomer 1), 141292-34-4; 3 (isomer 2), 141319-39-3; 4, 141292-33-3; [PPN][4], 141292-32-2; [PPN][5], 141292-36-6;  $[\text{Au}\{\text{P}(2\text{-Me-C}_6\text{H}_4)_3\}_2][5]$ , 141292-31-1; 6, 141292-28-6;  $[\text{Et}_3\text{NH}][\text{Fe}_4(\text{CO})_{12}\text{BHAuP}(2\text{-Me-C}_6\text{H}_4)_3]$ , 141319-38-2;  $\text{HFe}_4(\text{CO})_{12}\text{BHAu}\{\text{P}(c\text{-C}_6\text{H}_{11})_3\}$ , 141292-26-4;  $[\text{Et}_3\text{NH}][\text{HRu}_4(\text{CO})_{12}\text{BAuP}(2\text{-Me-C}_6\text{H}_4)_3]$ , 141319-36-0; [PPN][ $\{\text{HFe}_4(\text{CO})_{12}\text{BH}\}_2$ ], 108008-77-1;  $\{\text{P}(2\text{-Me-C}_6\text{H}_4)_3\}_2\text{PAuCl}$ , 83076-07-7;  $\{\text{P}(c\text{-C}_6\text{H}_{11})_3\}_2\text{PAuCl}$ , 49763-41-9; ClAu(dppm)AuCl, 37095-27-5; Au, 7440-57-5; Fe, 7439-89-6; Ru<sub>4</sub>(CO)<sub>12</sub>BAu<sub>3</sub>{P(2-Me-C<sub>6</sub>H<sub>4</sub>)<sub>3</sub>}<sub>2</sub>, 141292-29-7; Ru, 7440-18-8; [PPN][ $\{\text{HRu}_4(\text{CO})_{12}\text{BH}\}_2$ ], 125476-27-9.

**Supplementary Material Available:** Tables of bond distances, bond angles, thermal parameters, and H atom coordinates for 1,  $[\text{Au}(\text{PMePh}_2)_2][4]$ , and [PPN][5] (17 pages). Ordering information is given on any current masthead page.

OM9107707

## Gas-Phase Reactions of Molybdenum Oxide Ions with Small Hydrocarbons

Carolyn J. Cassady\*

Department of Chemistry, Miami University, Oxford, Ohio 45056

Stephen W. McElvany

Code 6113/Chemistry Division, Naval Research Laboratory, Washington, D.C. 20375-5000

Received October 25, 1991

The gas-phase ion/molecule reactions of Mo<sup>+</sup>, MoO<sup>+</sup>, and MoO<sub>2</sub><sup>+</sup> with small alkanes, alkenes, and C<sub>6</sub> hydrocarbons have been investigated using Fourier transform ion cyclotron resonance mass spectrometry. Product branching ratios and reaction rate constants are reported. Dehydrogenation dominates the reactions, with little cleavage of the strong Mo<sup>+</sup>-O and OMo<sup>+</sup>-O bonds. Aside from the production of MoO(CO)<sup>+</sup> from MoO<sub>2</sub><sup>+</sup> and ethene, no evidence is found for the formation of oxygenated hydrocarbons, either as neutral reaction products or as ligands bound to Mo<sup>+</sup>. However, the reactions of Mo<sup>+</sup>, MoO<sup>+</sup>, and MoO<sub>2</sub><sup>+</sup> differ in terms of both rates and pathways. In contrast to the slow reaction rates of the d<sup>5</sup> system Mo<sup>+</sup>, several MoO<sup>+</sup> and MoO<sub>2</sub><sup>+</sup> reactions proceed at or near the collision rate. Variations are also seen in product ion distributions, and for MoO<sub>2</sub><sup>+</sup>, unique reaction pathways involving dehydration and the elimination of small hydrocarbons occur. While Mo<sup>+</sup> and MoO<sup>+</sup> yield only products which are the result of C-H insertion, MoO<sub>2</sub><sup>+</sup> is capable of inserting into the C-C bonds of organic molecules.

### Introduction

Transition-metal oxides are common catalysts in oxidation processes. Oxygen atom transfer involving oxometal groups (M=O) plays a prominent role in these reactions. Although many transition-metal compounds can undergo oxygen transfer, molybdenum compounds are the most widely studied and employed. Over 100 oxygen-transfer reactions have been characterized for molybdenum compounds.<sup>1</sup> These involve a wide range of processes, including the epoxidation of alkenes<sup>2</sup> and alcohols,<sup>3</sup> the am-

moxidation of alkenes to nitriles,<sup>4</sup> the oxyhydration of alkenes to alcohols, aldehydes, and ketones,<sup>5</sup> the oxidative

(2) (a) Landau, R.; Sullivan, G. A.; Brown, D. *Chemtech* 1979, 9, 602.

(b) Mimoun, H.; Sere de Roch, I.; Sajus, L. *Tetrahedron* 1970, 26, 37.

(c) Chong, A. O.; Sharpless, K. B. *J. Org. Chem.* 1977, 42, 1587. (d) Daniel, C.; Keulka, G. W. *J. Catal.* 1972, 24, 529.

(3) Sharpless, K. B.; Verhoeven, T. R. *Aldrichim. Acta* 1979, 12, 63.

(4) (a) Reddy, B. M.; Narsimha, K.; Sivaraj, C.; Roa, P. K. *Appl. Catal.* 1989, 55, L1. (b) Burrington, J. D.; Kartisch, C. T.; Grasselli, R. K. *J. Catal.* 1983, 81, 489. (c) Burrington, J. D.; Kartisch, C. T.; Grasselli, R. K. *J. Catal.* 1984, 87, 363.

(5) (a) Tan, S.; Moro-oka, Y.; Ozaki, A. *J. Catal.* 1970, 17, 125. (b) Moro-oka, Y.; Takita, Y.; Ozaki, A. *J. Catal.* 1971, 23, 183. (c) Pitchai, R.; Klier, K. *Catal. Rev.* 1986, 28, 13. (d) Khan, M. M.; Somorjai, G. A. *J. Catal.* 1986, 28, 13.

(1) (a) Holm, R. H. *Chem. Rev.* 1987, 87, 1401. (b) Kung, H. H. *Transition Metal Oxides: Surface Chemistry and Catalysis*; Studies in Surface Science and Catalysis Series; Elsevier: New York, 1989; Vol. 45.

cleavage of aromatic systems,<sup>6</sup> and the oxidation of ketones to esters and lactones.<sup>7</sup> In addition to producing carbon-oxygen bonds, molybdenum compounds are utilized in the oxidation of functional groups containing nitrogen,<sup>8</sup> sulfur,<sup>9</sup> and phosphorus.<sup>10</sup> Another area that employs molybdenum oxides as catalysts is alkene metathesis,<sup>11</sup> isomerization,<sup>12</sup> and dehydrogenation.<sup>13</sup> Various photocatalytic processes in the oxidation of alkanes also involve molybdenum compounds.<sup>14</sup>

The importance of transition-metal oxides in the condensed phase has motivated several recent gas-phase studies. Over the past decade gas-phase transition-metal-ion chemistry has been an active area of research, providing information on the mechanistic, structural, thermodynamic, and kinetic aspects of inorganic processes.<sup>15</sup> For metal oxides, the reactions of  $\text{FeO}^+$ ,<sup>16</sup>  $\text{CrO}^+$ ,<sup>17,18</sup> and  $\text{VO}^+$ <sup>19</sup> with small hydrocarbons indicate that the extent of involvement of the oxo ligands in these gas-phase processes is dependent on the  $\text{M}^+-\text{O}$  bond strength. In addition, the reactions of  $\text{OsO}_y^+$  ( $y = 0-4$ )<sup>20</sup> with several small molecules and of  $\text{Co}_x\text{O}_y^+$ <sup>21</sup> with 2-methylpropane demonstrate that the oxygen-to-metal ratio affects the reaction pathways. Recent studies of molybdenum and tungsten oxide cluster anions with oxygen- and sulfur-containing compounds show that negative metal oxide ions also exhibit rich chemistries in the gas phase.<sup>22</sup>

Due to the importance of molybdenum compounds in condensed-phase oxidation processes, we chose to investigate molybdenum oxide chemistry in the gas phase. Although Schilling and Beauchamp have studied the reactions of  $\text{Mo}^+$  with hydrocarbons by ion beam mass spectrometric techniques,<sup>23</sup> the gas-phase reactions of molybdenum oxide cations have not previously been investigated. Here, we expand upon our recent study of the formation and dissociation of molybdenum oxide ions ( $\text{Mo}_x\text{O}_y^+/-$ )<sup>24</sup> by presenting the results of an investigation

of the gas-phase reactions of  $\text{Mo}^+$ ,  $\text{MoO}^+$ , and  $\text{MoO}_2^+$  with small hydrocarbons. Collision-induced dissociation (CID) and isotopic labeling experiments were used to gain information about reaction mechanisms and ion structures.

### Experimental Section

All experiments were performed using a Fourier transform ion cyclotron resonance mass spectrometer (FTMS)<sup>25</sup> that has been described in detail.<sup>26</sup> The mass spectrometer includes a Nicolet FTMS/1000 data system and a Nicolet 3-T superconducting magnet. The trapping plates of the 1-in. by 1-in. by 2-in. ( $z$ -axis) rectangular trapping cell are composed of 90% transparent nickel mesh. This allowed the frequency-doubled output of a Quanta-Ray DCR-2 Nd:YAG laser (532 nm, 1-10 mJ/pulse) to traverse the cell and vaporize the sample which was located on a direct inlet probe and inserted flush with one of the trapping plates.

$\text{Mo}^+$ ,  $\text{MoO}^+$ , and  $\text{MoO}_2^+$  were produced by direct laser vaporization of  $\text{MoO}_2$  or  $\text{MoO}_3$  as pressed pellets.<sup>24</sup> The <sup>92</sup>Mo isotope for a specific  $\text{MoO}_y^+$  was then isolated using resonance frequency ejection techniques.<sup>27</sup> To compensate for the wide range of internal energies that may be produced by laser vaporization<sup>28</sup> as well as translational energy that may have been imparted to the ions during the initial isolation process, the mass-selected ions underwent collisional cooling immediately following the laser pulse for ~500 ms with xenon gas at a static pressure of  $\sim 10^{-6}$  Torr or at a pulsed pressure with a maximum of  $10^{-5}$  Torr. The pulse of xenon was introduced into the vacuum chamber via a General Valve Corp. Series 9 pulsed solenoid valve<sup>29</sup> and was pumped away by an Edwards Diffstak Series 160 diffusion pump within 500 ms. The observed reaction rates of  $\text{MoO}_y^+$  with hydrocarbons generally increased as a result of this collisional cooling. Therefore, for each reaction, the xenon pressure or the time allowed for collisions was increased (i.e., the number of collisions was increased) until a linear pseudo-first-order reaction rate curve was obtained and the measured reaction rate remained constant. Following this thermalization period, the ions of interest were reisolated and allowed to react with a static pressure of hydrocarbon gas maintained at pressures up to  $1 \times 10^{-6}$  Torr, with typical operating pressures of  $<10^{-7}$  Torr.

The primary product ion branching ratios were reproducible to  $\pm 10\%$ . Rate constants were determined by observing the pseudo-first-order change in reactant ion intensity as a function of time at a constant hydrocarbon pressure. All reactions were studied to greater than 80% completion, and following collisional cooling, all first-order decay plots were linear, suggesting the predominance of ground-state reactant ions. Pressures were measured with a calibrated ion gauge<sup>30</sup> and were corrected for reactant gas ionization efficiency.<sup>31</sup> Errors in the pressure calibration factor and from other sources may render the absolute rate constants in error by as much as a factor of 2-3. Differences in relative rate constants should be significant, however, since they were measured under similar conditions.

Oxygen-exchange reactions employed static pressures of  $\text{H}_2^{18}\text{O}$  ( $>97\%$  <sup>18</sup>O, Isotec Inc.) on the order of  $10^{-7}$  Torr. CID experiments<sup>32</sup> utilized xenon collision gas at a static pressure of  $(1-5) \times 10^{-6}$  Torr. The collision energy was varied from 0 to 100 eV (laboratory).

(6) Dumas, T.; Bulani, W. *Oxidation of Petrochemicals: Chemistry and Technology*; Applied Science: London, 1974; p 53.

(7) Jacobson, S. E.; Tang, R.; Mares, F. *J. Chem. Soc., Chem. Commun.* 1978, 888.

(8) (a) Howe, G. R.; Hiatt, R. R. *J. Org. Chem.* 1970, 35, 4007. (b) Tolstikov, G. A.; Jemilev, U. M.; Jurjev, V. P.; Gershanov, F. B.; Rafikov, S. F. *Tetrahedron Lett.* 1977, 331.

(9) Schultz, H. S.; Freyermuth, H. B.; Buc, S. R. *J. Org. Chem.* 1963, 28, 1140.

(10) Hiatt, R.; McColeman, C. *Can. J. Chem.* 1971, 49, 1712.

(11) (a) Haines, R. J.; Leigh, G. *J. Chem. Soc. Rev.* 1975, 4, 155. (b) Calderon, N.; Lawrence, J. P.; Ofstead, E. A. *Adv. Organometal. Chem.* 1979, 17, 449. (c) Bailey, G. C. *Catal. Rev.* 1969, 3, 37.

(12) (a) Engelhardt, J.; Goldwasser, J.; Hall, W. K. *J. Catal.* 1981, 70, 364. (b) Goldwasser, J.; Engelhardt, J.; Hall, W. K. *J. Catal.* 1971, 70, 275.

(13) (a) Levin, V. A.; Vernova, T. V.; Tsailingol'd, A. L. *Kinet. Katal.* 1972, 13, 504. (b) Adams, C. *Ind. Eng. Chem.* 1969, 61, 30.

(14) (a) Pichat, P.; Herrmann, J.-M.; Disdier, J.; Mozzanega, M.-N. *J. Phys. Chem.* 1979, 83, 3122. (b) Marcinkowska, K.; Kaliaguine, S.; Roberge, P. *J. Catal.* 1984, 90, 49. (c) Awad, M. K.; Anderson, A. B. *J. Am. Chem. Soc.* 1990, 112, 1603.

(15) (a) Schulze, C.; Schwarz, H.; Peake, D. A.; Gross, M. L. *J. Am. Chem. Soc.* 1987, 109, 2368. (b) Allison, J. In *Progress in Inorganic Chemistry*; Lippard, S. J., Ed.; Wiley Interscience: New York, 1986; Vol. 34, p 628. (c) Buckner, S. W.; Freiser, B. S. *Polyhedron* 1988, 7, 1583.

(16) Jackson, T. C.; Jacobson, D. B.; Freiser, B. S. *J. Am. Chem. Soc.* 1984, 106, 1252.

(17) Kang, H.; Beauchamp, J. L. *J. Am. Chem. Soc.* 1986, 108, 5663.

(18) Kang, H.; Beauchamp, J. L. *J. Am. Chem. Soc.* 1986, 108, 7502.

(19) Jackson, T. C.; Carlin, T. J.; Freiser, B. S. *J. Am. Chem. Soc.* 1986, 108, 1120.

(20) Irikura, K. K.; Beauchamp, J. L. *J. Am. Chem. Soc.* 1989, 111, 75.

(21) Freas, R. B.; Campana, J. E. *J. Am. Chem. Soc.* 1986, 108, 4659.

(22) Maleknia, S.; Brodbelt, J.; Pope, K. *J. Am. Soc. Mass Spectrom.* 1991, 2, 212.

(23) Schilling, J. B.; Beauchamp, J. L. *Organometallics* 1988, 7, 194.

(24) Cassady, C. J.; Weil, D. A.; McElvany, S. W. *J. Chem. Phys.* 1992, 96, 691.

(25) A recent review of FTMS appears in: *Fourier Transform Mass Spectrometry: Evolution, Innovation, and Applications*; Buchanan, M. V., Ed.; ACS Symposium Series 359; American Chemical Society: Washington, DC, 1987.

(26) Parent, D. C.; McElvany, S. W. *J. Am. Chem. Soc.* 1989, 111, 2393.

(27) Comisarow, M. B.; Grassi, V.; Parisod, G. *Chem. Phys. Lett.* 1978, 57, 413.

(28) Kang, H.; Beauchamp, J. L. *J. Phys. Chem.* 1985, 89, 3364.

(29) Carlin, T. J.; Freiser, B. S. *Anal. Chem.* 1983, 55, 571.

(30) The ion gauge was calibrated using the reaction,  $\text{Kr}^+ + \text{CO}_2 \rightarrow \text{Kr} + \text{CO}_2^+$ , with rate constant information obtained from: Ikezoe, Y.; Matsuoka, S.; Takebe, M.; Viggiano, A. *Gas Phase Ion-Molecule Reaction Rate Constants through 1986*; Maruzen: Tokyo, 1987.

(31) Bartmess, J. E.; Georgiadis, R. M. *Vacuum* 1983, 33, 149.

(32) Cody, R. B.; Freiser, B. S. *Int. J. Mass Spectrom. Ion Phys.* 1982, 41, 199.

Table I. Primary Reactions of  $\text{MoO}_y^+$  ( $y = 0-2$ ) with Small Alkanes

hydrocarbon	products	rel abundance, %		
		$\text{Mo}^+$	$\text{MoO}^+$	$\text{MoO}_2^+$
methane		NR <sup>a</sup>	NR	NR
ethane	$k_{\text{obed}}$ , $\text{cm}^3 \text{s}^{-1}$	$<10^{-13}$	$<10^{-13}$	$<10^{-13}$
	$\text{MoO}_2\text{C}_2\text{H}_5^+ + 2\text{H}_2$	NR	5	0
	$\text{MoOC}_2\text{H}_4^+ + \text{H}_2$		95	100
propane	$k_{\text{obed}}$ , $\text{cm}^3 \text{s}^{-1}$	b	$6.7 \times 10^{-10}$	$2.3 \times 10^{-10}$
	$k_{\text{obed}}/k_{\text{Langevin}}^c$		0.66	0.23
	$\text{MoO}_2\text{C}_3\text{H}_7^+ + \text{C}_2\text{H}_4$	NR	0	20
	$\text{MoO}_2\text{C}_2\text{H}_5^+ + \text{CH}_4$		0	24
	$\text{MoOC}_3\text{H}_7^+ + 2\text{H}_2$		88	0
	$\text{MoO}_2\text{C}_3\text{H}_6^+ + \text{H}_2$		12	56
butane	$k_{\text{obed}}$ , $\text{cm}^3 \text{s}^{-1}$	b	$8.2 \times 10^{-10}$	$6.6 \times 10^{-10}$
	$k_{\text{obed}}/k_{\text{Langevin}}^c$		0.78	0.64
	$\text{MoO}_2\text{C}_4\text{H}_9^+ + \text{C}_2\text{H}_6$	0	6	16
	$\text{MoOC}_4\text{H}_9^+ + \text{H}_2\text{O} + \text{H}_2$	0	0	62
	$\text{MoO}_2\text{C}_3\text{H}_7^+ + \text{CH}_4$	0	0	15
	$\text{MoO}_2\text{C}_4\text{H}_8^+ + 2\text{H}_2$	100	94	0
	$\text{MoO}_2\text{C}_4\text{H}_7^+ + \text{H}_2$	0	0	7
	$k_{\text{obed}}$ , $\text{cm}^3 \text{s}^{-1}$	$3.8 \times 10^{-12}$	$9.8 \times 10^{-10}$	$8.8 \times 10^{-10}$
	$k_{\text{obed}}/k_{\text{Langevin}}^c$	0.0034	0.90	0.82
	2-methylpropane	$\text{MoOC}_4\text{H}_9^+ + \text{H}_2\text{O} + \text{H}_2$	0	0
$\text{MoOC}_3\text{H}_7^+ + \text{CH}_4 + \text{H}_2$		0	83	0
$\text{MoO}_2\text{C}_3\text{H}_6^+ + \text{CH}_4$		0	0	11
$\text{MoOC}_4\text{H}_8^+ + 2\text{H}_2$		0	8	0
$\text{MoO}_2\text{C}_4\text{H}_7^+ + \text{H}_2$		100	9	37
$k_{\text{obed}}$ , $\text{cm}^3 \text{s}^{-1}$		$1.6 \times 10^{-12}$	$1.0 \times 10^{-9}$	$5.3 \times 10^{-10}$
$k_{\text{obed}}/k_{\text{Langevin}}^c$		0.0014	0.92	0.50

<sup>a</sup>NR indicates that no reaction was observed. <sup>b</sup>The lack of reaction at hydrocarbon pressures on the order of  $10^{-7}$  Torr for reaction times of 5 s indicates that  $k_{\text{obed}} < 10^{-13} \text{ cm}^3 \text{ s}^{-1}$ . <sup>c</sup>Reaction efficiency. See ref 34.

## Results and Discussion

**Reactions of  $\text{Mo}^+$ ,  $\text{MoO}^+$ , and  $\text{MoO}_2^+$  with Deuterium.** The  $\text{MoO}_y^+$ ,  $y = 0-2$ , ions are unreactive with deuterium. In contrast, the third-row group 8 metal oxide ions  $\text{OsO}_y^+$ ,  $y = 1-3$ , react with hydrogen (and deuterium) to eliminate water (or deuterium oxide). This is believed to occur via a four-centered cycloaddition process.<sup>20</sup> If we assume that  $\text{MoO}^+$  and  $\text{MoO}_2^+$  do not produce deuterium oxide because the reaction is endothermic, this suggests that the  $\text{Mo}^+-\text{O}$  and  $\text{OMo}^+-\text{O}$  bond energies are greater than  $119 \text{ kcal mol}^{-1}$ .<sup>33</sup> Therefore, the  $\text{Mo}^+-\text{O}$  and  $\text{OMo}^+-\text{O}$  bonds may be stronger than their literature bond dissociation energies of  $114 \text{ kcal mol}^{-1}$ <sup>33</sup> indicate. However, upper and lower bond dissociation energies based on the presence or absence of ion/molecule reactions can only be assigned tentatively because the failure to observe a reaction may be due to factors other than overall reaction exothermicity (e.g., the presence of activation barriers or spin or orbital considerations).

**Reactions of  $\text{Mo}^+$  with Small Alkanes.** The reactions of  $\text{Mo}^+$  with small hydrocarbons were studied to provide a basis for direct comparisons of molybdenum oxide ion reactivity. The product ion distributions and rates for the reactions of  $\text{Mo}^+$ ,  $\text{MoO}^+$ , and  $\text{MoO}_2^+$  with  $\text{C}_1-\text{C}_4$  alkanes are summarized in Table I. Dehydrogenation is the only process observed in the reactions of  $\text{Mo}^+$  with small hydrocarbons. Extensive dehydrogenation has also been reported by Schilling and Beauchamp<sup>23</sup> in their investigation of  $\text{Mo}^+$  reactions with hydrocarbons using ion beam mass spectrometric techniques. This is consistent with many gas-phase studies which have shown that second- and third-row transition-metal ions preferentially activate C-H bonds (as opposed to C-C bonds).<sup>35-39</sup> Tolbert et

al. have explained this tendency in terms of the sizes and shapes of the orbitals used in bonding, with bonding in second- and third-row transition metals involving highly directional d orbitals that favor the symmetric, nondirectional hydrogen atom as opposed to a more directional carbon p orbital.<sup>35</sup>

Shilling et al. have studied  $\text{Mo}^+$  reactivity from experimental<sup>23</sup> and theoretical<sup>40</sup> standpoints. In terms of both the nature of the reaction pathways and the rates of reactions, they found the  $d^5$  system of  $\text{Mo}^+$  to be less reactive than most other atomic transition-metal cations. (However,  $\text{Mo}^+$  is considerably more reactive than its first-row group 6 neighbor  $\text{Cr}^+$ .<sup>23</sup>) A major reason for this is the relatively weak  $\text{Mo}^+-\text{H}$  and  $\text{Mo}^+-\text{C}_m\text{H}_n$  bonds, which lead to low reaction exothermicities during  $\text{Mo}^+$  bond activation of hydrocarbons. These bonds are known to be weak from both theoretical calculations<sup>40</sup> and the experimentally determined value of  $D(\text{Mo}^+-\text{H}) = 42 \pm 3 \text{ kcal mol}^{-1}$ .<sup>41</sup>

The atomic metal ion  $\text{Mo}^+$  does not react with methane. This is consistent with the ion beam results<sup>23</sup> and is expected because  $\text{Zr}^+$ ,<sup>42</sup> and the third-row transition-metal ions  $\text{Ta}^+$ ,<sup>38,39</sup>  $\text{W}^+$ ,<sup>43</sup>  $\text{Os}^+$ ,<sup>20</sup>  $\text{Ir}^+$ ,<sup>43</sup> and  $\text{Pt}^+$ <sup>43</sup> are the only

(35) (a) Tolbert, M.; Beauchamp, J. L. *J. Phys. Chem.* 1986, 90, 5015. (b) Tolbert, M. A.; Mandich, M. L.; Halle, L. F.; Beauchamp, J. L. *J. Am. Chem. Soc.* 1986, 108, 5675.

(36) (a) Sunderlin, L.; Aristov, N.; Armentrout, P. B. *J. Am. Chem. Soc.* 1987, 109, 78. (b) Sunderlin, L. S.; Armentrout, P. B. *J. Am. Chem. Soc.* 1989, 111, 3845.

(37) (a) Byrd, G. D.; Freiser, B. S. *J. Am. Chem. Soc.* 1982, 104, 5944. (b) Huang, Y.; Wise, M. B.; Jacobson, D. B.; Freiser, B. S. *Organometallics* 1987, 6, 346.

(38) Buckner, S. W.; MacMahon, T. J.; Byrd, G. D.; Freiser, B. S. *Inorg. Chem.* 1989, 28, 3511.

(39) Cassady, C. J.; McElvany, S. W. *J. Am. Chem. Soc.* 1990, 112, 4788.

(40) (a) Schilling, J. B.; Goddard, W. A., III; Beauchamp, J. L. *J. Am. Chem. Soc.* 1987, 109, 5565. (b) Schilling, J. B.; Goddard, W. A., III; Beauchamp, J. L. *J. Am. Chem. Soc.* 1987, 109, 5573. (c) Schilling, J. B.; Goddard, W. A., III; Beauchamp, J. L. *J. Phys. Chem.* 1987, 91, 4470.

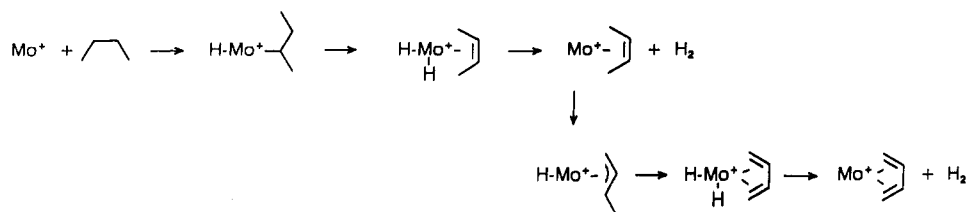
(41) Elkink, J. L.; Armentrout, P. B. *Inorg. Chem.* 1986, 25, 1080.

(42) Ransinghe, Y. A.; MacMahon, T. J.; Freiser, B. S. *J. Phys. Chem.* 1991, 95, 7721.

(33) Thermodynamic values were taken and derived from: Lias, S. G.; Bartmess, J. F.; Liebman, J. F.; Holmes, J. L.; Levin, R. D.; Mallard, W. G. *J. Phys. Chem. Ref. Data* 1988, 17 (Suppl. 1).

(34) Su, T.; Bowers, M. T. In *Gas Phase Ion Chemistry*; Bowers, M. T., Ed.; Academic Press: New York, 1979; Chapter 3.

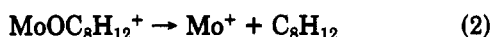
Scheme I



ground-state atomic metal ions that are known to react exothermically with  $\text{CH}_4$ . Ethane and propane also did not react with  $\text{Mo}^+$  in the present FTMS study. In contrast,  $\text{Mo}^+$  eliminated one and two molecules of  $\text{H}_2$  from both ethane and propane in the ion beam study.<sup>23</sup> However, the cross sections for these reactions were very low, suggesting that they are near thermoneutral or possibly slightly endothermic.<sup>23</sup> This implies that  $D(\text{Mo}^+-\text{C}_2\text{H}_4)$  and  $D(\text{Mo}^+-\text{C}_3\text{H}_6)$  are less than or equal to 33 and 30 kcal/mol, respectively.<sup>33</sup>

The  $\text{Mo}^+$  ions react with *n*-butane to produce  $\text{MoC}_4\text{H}_6^+$  via the elimination of two molecules of  $\text{H}_2$ . This agrees with the ion beam study.<sup>23</sup> This process has a rate constant of  $3.8 \times 10^{-12} \text{ cm}^3 \text{ s}^{-1}$ , which is extremely slow relative to the Langevin collision frequency of  $1.1 \times 10^{-9} \text{ cm}^3 \text{ s}^{-1}$ . As shown in Scheme I, this reaction can be envisioned as proceeding through a mechanism involving  $\text{Mo}^+$  insertion into a C-H bond, followed by a  $\beta$ -hydride shift and the reductive elimination of  $\text{H}_2$ . This yields a  $\text{Mo}^+$ -butene complex that eliminates a second molecule of  $\text{H}_2$ . This is an established mechanism which has been applied in numerous metal ion reactions with organic molecules.<sup>15</sup> It has been discussed in detail by Schilling and Beauchamp for the reactions of  $\text{Mo}^+$  with hydrocarbons.<sup>23</sup>

The secondary reactions of  $\text{MoC}_m\text{H}_n^+$  are shown in Table II. The product ion from the  $\text{Mo}^+$  and *n*-butane reaction,  $\text{MoC}_4\text{H}_6^+$ , also reacts with *n*-butane by double dehydrogenation to form  $\text{MoC}_3\text{H}_{12}^+$ . In contrast to the slow rate of the primary reaction, this secondary process occurs near the collision rate. This may be due to the fact that, with the addition of a ligand,  $\text{Mo}^+$  loses its extremely stable  $d^5$  character. CID studies of  $\text{MoC}_8\text{H}_{12}^+$  yield  $\text{MoC}_6\text{H}_8^+$  as the major low-energy dissociation product, with  $\text{Mo}^+$  forming at higher energies, reactions 1 and 2.



The absence of  $\text{MoC}_4\text{H}_6^+$  as a CID product suggests that  $\text{MoC}_8\text{H}_{12}^+$  contains an intact  $\text{C}_8\text{H}_y$  ligand as opposed to two  $\text{C}_4\text{H}_6$  ligands. Similar ligand-coupling processes dominate the reactions of  $\text{Ta}^+$ <sup>38,39</sup> and  $\text{Nb}^+$ <sup>38</sup> with hydrocarbons.

Loss of a single molecule of  $\text{H}_2$  occurs in the reaction of 2-methylpropane with  $\text{Mo}^+$ . In the ion beam study,  $\text{Mo}^+$  reacted with 2-methylpropane via the elimination of one and two molecules of  $\text{H}_2$  at 37% and 63%, respectively.<sup>23</sup> This suggests that the  $\text{H}_2$  loss product ions,  $\text{MoC}_4\text{H}_8^+$ , in the ion beam experiment have more energy than in the FTMS experiment and that this energy leads to elimination of a second  $\text{H}_2$  molecule.

In our FTMS experiments, the reactions of  $\text{Mo}^+$  with *n*-butane and 2-methylpropane are extremely slow, with efficiencies of 0.0034 and 0.0014, respectively. That is, only approximately 1 out of every 1000 collisions results in a reaction. In the ion beam study of Schilling and Beauchamp, the reaction efficiencies were 0.031 and 0.012 for

Table II. Secondary Reactions of  $\text{MoC}_m\text{H}_n^+$  with Hydrocarbons

hydrocarbon	reactant ion	products	rel abundance, %
butane	$\text{MoC}_4\text{H}_6^+$	$\text{MoC}_8\text{H}_{12}^+ + 2\text{H}_2$	100
	$\text{MoC}_4\text{H}_8^+$	$\text{MoC}_8\text{H}_{14}^+ + 2\text{H}_2$	100
2-methylpropane	$\text{MoC}_3\text{H}_4^+$	$\text{MoC}_6\text{H}_8^+ + 2\text{H}_2$	25
	$\text{MoC}_3\text{H}_6^+$	$\text{MoC}_6\text{H}_8^+ + \text{H}_2$	75
propene	$\text{MoC}_6\text{H}_8^+$	$\text{MoC}_9\text{H}_{10}^+ + 2\text{H}_2$	70
	$\text{MoC}_6\text{H}_8^+$	$\text{MoC}_9\text{H}_{10}^+ + \text{H}_2$	30
	$\text{MoC}_6\text{H}_8^+$	$\text{MoC}_9\text{H}_{10}^+ + 3\text{H}_2$	70
	$\text{MoC}_6\text{H}_8^+$	$\text{MoC}_9\text{H}_{10}^+ + 2\text{H}_2$	30
	$\text{MoC}_9\text{H}_{8,10}^{+a}$	$\text{MoC}_{12}\text{H}_{10}^+$	20
	$\text{MoC}_9\text{H}_{8,10}^{+a}$	$\text{MoC}_{12}\text{H}_{12}^+$	80
	$\text{MoC}_{12}\text{H}_{10}^+$	$\text{MoC}_{15}\text{H}_{16}^+$	100
	$\text{MoC}_4\text{H}_6^+$	$\text{MoC}_8\text{H}_8^+ + 3\text{H}_2$	75
1-butene	$\text{MoC}_4\text{H}_6^+$	$\text{MoC}_8\text{H}_{10}^+ + 2\text{H}_2$	25
	$\text{MoC}_4\text{H}_6^+$	$\text{MoC}_8\text{H}_{10}^+ + \text{H}_2$	35
	$\text{MoC}_8\text{H}_{8,10}^{+a}$	$\text{MoC}_{11}\text{H}_{12}^+$	50
	$\text{MoC}_8\text{H}_{8,10}^{+a}$	$\text{MoC}_{12}\text{H}_{12}^+$	15
cis-2-butene	$\text{MoC}_4\text{H}_6^+$	$\text{MoC}_8\text{H}_8^+ + 3\text{H}_2$	80
	$\text{MoC}_4\text{H}_6^+$	$\text{MoC}_8\text{H}_{10}^+ + 2\text{H}_2$	20
	$\text{MoC}_8\text{H}_{8,10}^{+a}$	$\text{MoC}_{11}\text{H}_{12}^+$	25
	$\text{MoC}_8\text{H}_{8,10}^{+a}$	$\text{MoC}_{12}\text{H}_{12}^+$	60
	$\text{MoC}_8\text{H}_{8,10}^{+a}$	$\text{MoC}_{12}\text{H}_{14}^+$	15
	$\text{MoC}_8\text{H}_{8,10}^{+a}$	$\text{MoC}_{12}\text{H}_{14}^+$	15
2-methylpropene	$\text{MoC}_4\text{H}_6^+$	$\text{MoC}_8\text{H}_8^+ + 3\text{H}_2$	45
	$\text{MoC}_4\text{H}_6^+$	$\text{MoC}_8\text{H}_{10}^+ + 2\text{H}_2$	45
	$\text{MoC}_8\text{H}_8^+$	$\text{MoC}_9\text{H}_{12}^+ + \text{H}_2$	10
	$\text{MoC}_8\text{H}_8^+$	$\text{MoC}_{12}\text{H}_{12}^+ + 2\text{H}_2$	65
	$\text{MoC}_8\text{H}_{10}^+$	$\text{MoC}_{12}\text{H}_{14}^+ + \text{H}_2$	35
	$\text{MoC}_8\text{H}_{10}^+$	$\text{MoC}_{12}\text{H}_{14}^+ + 2\text{H}_2$	75
	$\text{MoC}_8\text{H}_{10}^+$	$\text{MoC}_{12}\text{H}_{16}^+ + \text{H}_2$	25
	$\text{MoC}_8\text{H}_{10}^+$	$\text{MoC}_{12}\text{H}_{16}^+ + 4\text{H}_2$	10
<i>n</i> -hexane	$\text{MoC}_6\text{H}_{10}^+$	$\text{MoC}_{12}\text{H}_{18}^+ + 3\text{H}_2$	90
cyclohexane	$\text{MoC}_6\text{H}_8^+$	$\text{MoC}_{12}\text{H}_{12}^+ + 3\text{H}_2$	100
cyclohexane	$\text{MoC}_6\text{H}_8^+$	$\text{MoC}_{12}\text{H}_{12}^+ + 2\text{H}_2$	100

<sup>a</sup> Due to low intensities, the two reactant ions were not isolated individually. Therefore, the product ions and relative abundances reported are a result of a combination of the reactions of both ions.

*n*-butane and 2-methylpropane, respectively.<sup>44</sup> While the reactions are still very slow, these values are a factor of 10 higher than in the FTMS studies. This may indicate that the  $\text{Mo}^+$  reactions with  $\text{C}_3$  and  $\text{C}_4$  alkanes are near thermoneutral and that small differences in ion internal energy can have a relatively large effect on the observed rates of reactions and, as the 2-methylpropane reaction suggests, on product formation.

**Reactions of  $\text{Mo}^+$  with Small Alkenes.** Table III summarizes the reactions of  $\text{Mo}^+$ ,  $\text{MoO}^+$ , and  $\text{MoO}_2^+$  with  $\text{C}_2$ - $\text{C}_4$  alkenes. In the present FTMS study,  $\text{Mo}^+$  does not react with ethene. The ion beam study showed dehydrogenation of ethene by  $\text{Mo}^+$ , but this process occurred with a very low reaction cross section, suggesting that it is near thermoneutral or slightly endothermic.<sup>23</sup> The FTMS results indicate that  $D(\text{Mo}^+-\text{C}_2\text{H}_2) \leq 42$  kcal/mol.<sup>33</sup>

Elimination of a single  $\text{H}_2$  molecule dominates the reactions of  $\text{Mo}^+$  with  $\text{C}_3$  and  $\text{C}_4$  alkenes. These reactions

(43) Irikura, K. K.; Beauchamp, J. L. *J. Am. Chem. Soc.* 1991, 113, 2769.

(44) Reaction efficiencies for the data reported in ref 23 were obtained by calculating the ratios of the experimental cross sections to the theoretical Langevin cross sections. The method for calculating the Langevin cross sections is discussed in ref 18.

Table III. Primary Reactions of  $\text{MoO}_y^+$  ( $y = 0-2$ ) with Small Alkenes

hydrocarbon	products	rel abundance, %		
		$\text{Mo}^+$	$\text{MoO}^+$	$\text{MoO}_2^+$
ethene	$\text{MoOC}_2\text{H}_2^+ + \text{H}_2\text{O}$	NR <sup>a</sup>	0	36
	$\text{MoO}_2\text{C}^+ + \text{CH}_4$		0	64
	$\text{MoOC}_2\text{H}_2^+ + \text{H}_2$		100	0
	$k_{\text{obed}}, \text{cm}^3 \text{s}^{-1}$	<i>b</i>	$1.1 \times 10^{-9}$	$3.8 \times 10^{-10}$
	$k_{\text{obed}}/k_{\text{Langevin}}^c$		1.0	0.37
propene	$\text{MoO}_2\text{CH}_4^+ + \text{C}_2\text{H}_2$	0	0	28
	$\text{MoOC}_3\text{H}_4^+ + \text{H}_2\text{O}$	0	0	23
	$\text{MoOC}_2\text{H}_2^+ + \text{CH}_4$	0	7	0
	$\text{MoO}_y\text{C}_3\text{H}_4^+ + \text{H}_2$	100	93	49
	$k_{\text{obed}}, \text{cm}^3 \text{s}^{-1}$	$2.8 \times 10^{-10}$	$9.4 \times 10^{-10}$	$7.7 \times 10^{-10}$
	$k_{\text{obed}}/k_{\text{Langevin}}$	0.26	0.90	0.75
1-butene	$\text{MoO}_2\text{C}_2\text{H}_2^+ + \text{C}_2\text{H}_6$	0	0	9
	$\text{MoO}_2\text{C}_2\text{H}_4^+ + \text{C}_2\text{H}_4$	0	0	51
	$\text{MoOC}_4\text{H}_4^+ + \text{H}_2\text{O} + \text{H}_2$	0	0	10
	$\text{MoOC}_4\text{H}_6^+ + \text{H}_2\text{O}$	0	0	13
	$\text{MoO}_2\text{C}_3\text{H}_4^+ + \text{CH}_4$	0	0	3
	$\text{MoO}_2\text{C}_3\text{H}_6^+ + \text{CH}_2$	0	0	4
	$\text{MoO}_y\text{C}_4\text{H}_4^+ + 2\text{H}_2$	6	90	5
	$\text{MoO}_y\text{C}_4\text{H}_6^+ + \text{H}_2$	94	10	5
	$k_{\text{obed}}, \text{cm}^3 \text{s}^{-1}$	$9.8 \times 10^{-10}$	$1.2 \times 10^{-9}$	$1.2 \times 10^{-9}$
	$k_{\text{obed}}/k_{\text{Langevin}}$	0.88	1.1	1.1
	cis-2-butene	$\text{MoO}_2\text{C}_2\text{H}_2^+ + \text{C}_2\text{H}_6$	0	0
$\text{MoO}_2\text{C}_2\text{H}_4^+ + \text{C}_2\text{H}_4$		0	0	67
$\text{MoOC}_4\text{H}_4^+ + \text{H}_2\text{O} + \text{H}_2$		0	0	12
$\text{MoOC}_4\text{H}_6^+ + \text{H}_2\text{O}$		0	0	12
$\text{MoO}_y\text{C}_4\text{H}_4^+ + 2\text{H}_2$		9	95	0
$\text{MoO}_y\text{C}_4\text{H}_6^+ + \text{H}_2$		91	5	0
$k_{\text{obed}}, \text{cm}^3 \text{s}^{-1}$		$6.8 \times 10^{-10}$	$1.1 \times 10^{-9}$	$8.7 \times 10^{-10}$
$k_{\text{obed}}/k_{\text{Langevin}}$		0.61	1.0	0.82
2-methylpropene	$\text{MoO}_2\text{CH}_4^+ + \text{C}_3\text{H}_4$	0	0	15
	$\text{MoO}_2\text{C}_2\text{H}_4^+ + \text{C}_2\text{H}_4$	0	0	51
	$\text{MoOC}_4\text{H}_4^+ + \text{H}_2\text{O} + \text{H}_2$	0	0	19
	$\text{MoO}_y\text{C}_4\text{H}_6^+ + \text{H}_2\text{O}$	0	5	8
	$\text{MoO}_y\text{C}_3\text{H}_4^+ + \text{CH}_4$	0	50	7
	$\text{MoOC}_4\text{H}_4^+ + 2\text{H}_2$	0	29	0
	$\text{MoO}_y\text{C}_4\text{H}_6^+ + \text{H}_2$	100	16	0
	$k_{\text{obed}}, \text{cm}^3 \text{s}^{-1}$	$8.3 \times 10^{-10}$	$1.2 \times 10^{-9}$	$1.2 \times 10^{-9}$
	$k_{\text{obed}}/k_{\text{Langevin}}$	0.74	1.1	1.1

<sup>a</sup> NR indicates that no reaction was observed. <sup>b</sup> The lack of reaction at hydrocarbon pressures on the order of  $10^{-7}$  Torr for reaction times of 5 s indicates that  $k_{\text{obed}} < 10^{-13} \text{ cm}^3 \text{ s}^{-1}$ . <sup>c</sup> Reaction efficiency. See ref 34.

occur readily with rates that approach the Langevin collision frequency. For the facile alkene reactions, our FTMS reaction efficiencies agree with the ion beam reaction efficiencies to within a factor of 2 (with the ion beam efficiencies being generally higher);<sup>44</sup> this is well within the experimental errors associated with the two techniques. Schilling and Beauchamp<sup>23</sup> have suggested that  $\text{Mo}^+$  is more reactive with alkenes than with alkanes because of interaction between  $\text{Mo}^+$  and the alkene  $\pi$  system. These reactions can be envisioned as proceeding through the established mechanism for the reactions of metal ions with alkenes. This involves  $\text{Mo}^+$  insertion into an allylic C-H bond, followed by a  $\beta$ -H transfer and the reductive elimination of  $\text{H}_2$ .<sup>23,45</sup>

Numerous secondary reactions are observed between  $\text{MoC}_m\text{H}_n^+$  and alkenes. For example, a sequence of reactions occur between  $\text{Mo}^+$  and propene (Table II), with the end result being the formation of  $\text{MoC}_{12}\text{H}_{12}^+$  and  $\text{MoC}_{16}\text{H}_{16}^+$  from the reactions of four and five propene molecules, respectively. These processes involve only dehydrogenation. CID studies were performed on the most abundant  $\text{MoC}_m\text{H}_n^+$  species.  $\text{MoC}_3\text{H}_4^+$ ,  $\text{MoC}_6\text{H}_8^+$ , and  $\text{MoC}_9\text{H}_8^+$  eliminate  $\text{H}_2$  as the lowest energy CID product, with loss of the entire  $\text{C}_m\text{H}_n$  ligand dominating at higher energies. This suggests that ligand coupling has occurred,

leading to one intact  $\text{C}_m\text{H}_n$  attached to  $\text{Mo}^+$ .  $\text{MoC}_6\text{H}_8^+$  dissociates to yield only  $\text{Mo}^+$ , which implies a  $\text{Mo}^+$ -benzene structure. This is supported by the fact that  $\text{MoC}_6\text{H}_8^+$  produced from cyclohexene also fragments to yield only  $\text{Mo}^+$ .  $\text{MoC}_{12}\text{H}_{12}^+$  is unique, forming  $\text{MoC}_{12}\text{H}_{10}^+$  (a minor product),  $\text{MoC}_6\text{H}_8^+$ , and  $\text{Mo}^+$  as CID products at progressively higher energies, reactions 3-5. This is



identical to the fragmentation of  $\text{MoC}_{12}\text{H}_{12}^+$  produced from the reaction of  $\text{Mo}^+$  with two molecules of cyclohexene. These results are consistent with the attachment of two benzene ligands to  $\text{Mo}^+$ . Similar CID processes have been observed for  $\text{NbC}_{12}\text{H}_{12}^+$ <sup>38</sup> and  $\text{TaC}_{12}\text{H}_{12}^+$ .<sup>38,39</sup>

The  $\text{Mo}^+$  ions react with 1-butene and cis-2-butene by primarily elimination of a single  $\text{H}_2$ . In both instances, minor amounts of  $2\text{H}_2$  loss are observed. Additional reactions of the primary product ions with the butene isomers yield  $\text{MoC}_{12}\text{H}_{12}^+$  as the major product with lesser amounts of  $\text{MoC}_{11}\text{H}_{12}^+$  and  $\text{MoC}_{12}\text{H}_{14}^+$  forming. The production of  $\text{MoC}_{11}\text{H}_{12}^+$  must involve a C-C bond cleavage and the elimination of methane. CID of the product ions involves primarily  $\text{H}_2$  elimination, as well as the formation of  $\text{Mo}^+$  via elimination of the entire  $\text{C}_m\text{H}_n$  ligand. This is again consistent with structures containing one intact  $\text{C}_m\text{H}_n$  ligand. The exception to this trend is

(45) (a) Jacobson, D. B.; Freiser, B. S. *J. Am. Chem. Soc.* 1983, 105, 7484. (b) Armentrout, P. B.; Halle, L. F.; Beauchamp, J. L. *J. Am. Chem. Soc.* 1981, 103, 6624.

Table IV. Primary Reactions of  $\text{MoO}_y^+$  ( $y = 0-2$ ) with Selected  $\text{C}_6$  Hydrocarbons

hydrocarbon	products	rel abundance, %		
		$\text{Mo}^+$	$\text{MoO}^+$	$\text{MoO}_2^+$
<i>n</i> -hexane	$\text{MoOC}_4\text{H}_8^+ + \text{C}_2\text{H}_6 + \text{H}_2\text{O}$	0	0	21
	$\text{MoO}_2\text{C}_3\text{H}_6^+ + \text{C}_3\text{H}_8$	0	0	27
	$\text{MoOC}_4\text{H}_8^+ + \text{C}_2\text{H}_6 + \text{H}_2$	0	42	0
	$\text{MoO}_2\text{C}_4\text{H}_8^+ + \text{C}_2\text{H}_6$	0	0	43
	$\text{MoOC}_6\text{H}_8^+ + 4\text{H}_2$	0	47	0
	$\text{MoOC}_6\text{H}_8^+ + 3\text{H}_2$	0	11	0
	$\text{MoO}_y\text{C}_6\text{H}_{10}^+ + 2\text{H}_2$	100	0	9
	$k_{\text{obsd}}, \text{cm}^3 \text{s}^{-1}$	$2.0 \times 10^{-10}$	$1.2 \times 10^{-9}$	$1.1 \times 10^{-9}$
	$k_{\text{obsd}}/k_{\text{Langevin}}^a$	0.17	1.0	0.97
	cyclohexane	$\text{MoOC}_6\text{H}_8^+ + \text{H}_2\text{O} + 2\text{H}_2$	0	0
$\text{MoO}_y\text{C}_6\text{H}_8^+ + 3\text{H}_2$		100	100	3
$\text{MoO}_2\text{C}_6\text{H}_8^+ + 2\text{H}_2$		0	0	6
$k_{\text{obsd}}, \text{cm}^3 \text{s}^{-1}$		$5.8 \times 10^{-11}$	$1.2 \times 10^{-9}$	$1.0 \times 10^{-9}$
$k_{\text{obsd}}/k_{\text{Langevin}}$		0.049	1.1	0.91
cyclohexene	$\text{MoOC}_6\text{H}_8^+ + \text{H}_2\text{O} + \text{H}_2$	0	0	58
	$\text{MoO}_y\text{C}_6\text{H}_8^+ + 2\text{H}_2$	100	100	42
	$k_{\text{obsd}}, \text{cm}^3 \text{s}^{-1}$	$8.9 \times 10^{-10}$	$9.7 \times 10^{-10}$	$9.4 \times 10^{-10}$
	$k_{\text{obsd}}/k_{\text{Langevin}}$	0.76	0.86	0.86

<sup>a</sup> Reaction efficiency. See ref 34.

$\text{MoC}_{12}\text{H}_{12}^+$ , which undergoes CID in the manner discussed above and is probably a dibenzene species.

Single  $\text{H}_2$  elimination is the only process occurring between  $\text{Mo}^+$  with 2-methylpropene. Dehydrogenation is again the dominant pathway in the secondary reactions, with  $\text{MoC}_{12}\text{H}_{14}^+$  and  $\text{MoC}_{12}\text{H}_{16}^+$  being the major terminal products. Several minor products, such as  $\text{MoC}_9\text{H}_{12}^+$ ,  $\text{MoC}_{10}\text{H}_{12}^+$ , and  $\text{MoC}_{11}\text{H}_{12}^+$ , are also observed and indicate that C-C bond cleavage is occurring to a limited extent in the secondary reactions.

**Reactions of  $\text{Mo}^+$  with Selected  $\text{C}_6$  Hydrocarbons.** The importance of  $\text{MoC}_6\text{H}_8^+$  and  $\text{MoC}_{12}\text{H}_{12}^+$  in the  $\text{Mo}^+$  reactions with small alkanes and alkenes prompted an investigation of the  $\text{Mo}^+$  reactions with cyclohexane and cyclohexene. For comparison purposes, *n*-hexane was also studied. These results are given in Table IV.

The reactions of  $\text{Mo}^+$  with both cyclohexane and cyclohexene produce exclusively  $\text{MoC}_6\text{H}_8^+$ . As expected, cyclohexene reacts much faster ( $k_{\text{obsd}} = 8.0 \times 10^{-10} \text{ cm}^3 \text{ s}^{-1}$ ) than cyclohexane ( $k_{\text{obsd}} = 5.9 \times 10^{-11} \text{ cm}^3 \text{ s}^{-1}$ ). The only CID process for  $\text{MoC}_6\text{H}_8^+$  is the elimination of  $\text{C}_6\text{H}_8$  to form  $\text{Mo}^+$ . This provides strong evidence for a  $\text{Mo}^+$ -benzene structure.  $\text{MoC}_6\text{H}_8^+$  reacts with cyclohexane and cyclohexene at near the collision rate to produce  $\text{MoC}_{12}\text{H}_{12}^+$ . Dissociation of this ion to  $\text{MoC}_6\text{H}_8^+$  at low energies and  $\text{Mo}^+$  at high energies corroborates the dibenzene structure.

The reaction of  $\text{Mo}^+$  with *n*-hexane is quite different from the reactions with cyclic  $\text{C}_6$  hydrocarbons. The only product is  $\text{MoC}_6\text{H}_{10}^+$ , produced by double dehydrogenation. While this reaction is slow relative to the collision rate ( $k_{\text{obsd}}/k_{\text{Langevin}} = 0.17$ ), it is considerably faster than the reactions of  $\text{Mo}^+$  with smaller alkanes. The FTMS reaction efficiency agrees well with the ion beam reaction efficiency of 0.16;<sup>44</sup> however, the ion beam studied yielded products resulting from losses of one, two, three, and four molecules of  $\text{H}_2$ .<sup>23</sup> Ion energetics may again account for the differences in product formation. In our study, the lone product,  $\text{MoC}_6\text{H}_{10}^+$ , reacts with one additional molecule of *n*-hexane, producing only dehydrogenation products which do not react further.

**Reactions of  $\text{MoO}^+$  with Small Alkanes.** The addition of an oxygen atom to  $\text{Mo}^+$  frees the metal species from the reactivity constraints of a half-filled d orbital. Thus,  $\text{MoO}^+$  reacts much more readily than  $\text{Mo}^+$ . Table I contains product ion distributions and rates for the reactions of  $\text{MoO}^+$  with alkanes, while the secondary reac-

Table V. Secondary Reactions of  $\text{MoOC}_m\text{H}_n^+$  with Hydrocarbons

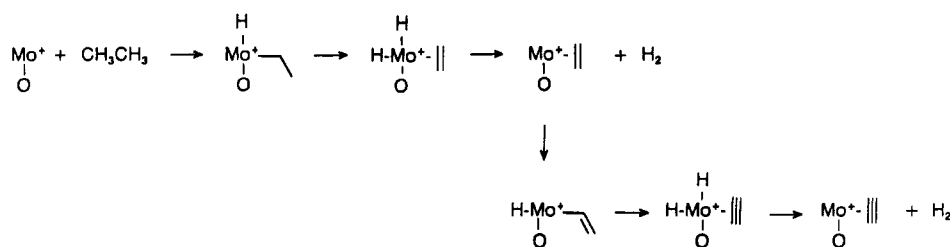
hydrocarbon	reactant ion	products	rel abundance, %
ethane	$\text{MoOC}_2\text{H}_2^+$	$\text{MoOC}_4\text{H}_6^+ + \text{H}_2$	100
	$\text{MoOC}_2\text{H}_4^+$	$\text{MoOC}_4\text{H}_8^+ + \text{H}_2$	100
propane	$\text{MoOC}_3\text{H}_4^+$	$\text{MoOC}_4\text{H}_6^+ + \text{C}_2\text{H}_6$	60
		$\text{MoOC}_4\text{H}_8^+ + \text{C}_2\text{H}_4$	40
2-methylpropane	$\text{MoOC}_3\text{H}_4^+$	$\text{MoOC}_5\text{H}_{10}^+ + \text{C}_2\text{H}_6$	65
		$\text{MoOC}_5\text{H}_{10}^+ + \text{C}_2\text{H}_4$	35
	$\text{MoOC}_4\text{H}_6^+$	$\text{MoOC}_5\text{H}_{12}^+ + \text{C}_3\text{H}_8$	40
		$\text{MoC}_8\text{H}_{16}^+ + \text{H}_2\text{O}$	60
ethene	$\text{MoOC}_2\text{H}_2^+{}^a$	$\text{MoOC}_4\text{H}_6^+ + \text{H}_2$	100
	$\text{MoOC}_4\text{H}_4^+$	$\text{MoOC}_6\text{H}_8^+ + \text{H}_2$	100
	$\text{MoOC}_6\text{H}_6^+$	$\text{MoOC}_8\text{H}_{10}^+ + \text{H}_2$	100
	$\text{MoOC}_8\text{H}_8^+$	$\text{MoOC}_{10}\text{H}_{10}^+ + \text{H}_2$	100
	$\text{MoOC}_2\text{H}_4^+$	$\text{MoOC}_4\text{H}_6^+ + \text{H}_2$	100
propene	$\text{MoOC}_2\text{H}_2^+$	$\text{MoOC}_5\text{H}_8^+ + \text{H}_2$	100
	$\text{MoOC}_3\text{H}_4^+{}^a$	$\text{MoOC}_4\text{H}_6^+ + \text{C}_2\text{H}_6$	15
		$\text{MoOC}_4\text{H}_8^+ + \text{C}_2\text{H}_4$	50
		$\text{MoOC}_6\text{H}_8^+ + 2\text{H}_2$	35
1-butene	$\text{MoOC}_4\text{H}_6^+$	$\text{MoOC}_5\text{H}_8^+ + \text{C}_2\text{H}_4$ <sup>b</sup>	80
		$\text{MoOC}_7\text{H}_8^+ + 2\text{H}_2$ <sup>b</sup>	20
	$\text{MoOC}_4\text{H}_4^+$	$\text{MoOC}_6\text{H}_8^+ + \text{C}_2\text{H}_6$	25
		$\text{MoOC}_7\text{H}_8^+ + \text{CH}_4$	20
		$\text{MoOC}_9\text{H}_8^+ + 2\text{H}_2$	35
<i>cis</i> -2-butene	$\text{MoOC}_4\text{H}_4^+$	$\text{MoOC}_8\text{H}_{10}^+ + \text{H}_2$	20
		$\text{MoOC}_6\text{H}_8^+ + \text{C}_2\text{H}_6$ <sup>c</sup>	20
		$\text{MoOC}_6\text{H}_8^+ + \text{C}_2\text{H}_4$ <sup>c</sup>	5
		$\text{Mo}_2\text{H}_{10}^+ + \text{C}_2\text{H}_2$ <sup>c</sup>	15
		$\text{MoOC}_7\text{H}_8^+ + \text{C}_2\text{H}_4$ <sup>c</sup>	15
2-methylpropene		$\text{MoOC}_8\text{H}_8^+ + 2\text{H}_2$ <sup>c</sup>	15
		$\text{MoOC}_8\text{H}_{10}^+ + \text{H}_2$ <sup>c</sup>	30

<sup>a</sup> Ions originally produced from both  $\text{MoO}^+$  and  $\text{MoO}_2^+$  react in a similar manner with the neutral. <sup>b</sup> These ions continue to react with propene to eventually yield  $\text{MoOC}_8\text{H}_{10}^+$ ,  $\text{MoOC}_9\text{H}_{10}^+$ , and  $\text{MoOC}_{12}\text{H}_{18}^+$ . <sup>c</sup> These ions continue to react with *cis*-2-butene to yield  $\text{MoC}_{12}\text{H}_8^+$ ,  $\text{MoC}_{12}\text{H}_{10}^+$ , and  $\text{MoOC}_{12}\text{H}_8^+$ . <sup>d</sup> The four primary products from the  $\text{MoO}^+$  and 2-methylpropene reaction each underwent several secondary reactions. These product ions, in turn, were also reactive. Due to the extreme complexity of the spectra, the isolation of reaction pathways was not performed.

tions of  $\text{MoOC}_m\text{H}_n^+$  are reported in Table V.

The extensive dehydrogenation that occurs in  $\text{Mo}^+$  reactions with hydrocarbons is also observed for  $\text{MoO}^+$ . However, as the reactions with 2-methylpropane and *n*-hexane demonstrate, C-C bond cleavage also plays a role in the  $\text{MoO}^+$  reactions. The  $\text{Mo}^+-\text{O}$  bond is strong, with a bond energy of at least 114 kcal mol<sup>-1</sup>.<sup>33</sup> As the results

Scheme II



in Tables I, III, and IV indicate, this bond is rarely cleaved in the reactions of  $\text{MoO}^+$  with hydrocarbons.  $\text{VO}^+$ , which has a bond energy of  $131 \text{ kcal mol}^{-1}$ ,<sup>46</sup> also does not cleave during reactions with hydrocarbons. In contrast, the weaker  $\text{Os}^+-\text{O}$  ( $D = 100 \pm 12 \text{ kcal mol}^{-1}$ ),<sup>20</sup>  $\text{Cr}^+-\text{O}$  ( $D = 85.3 \pm 1.3 \text{ kcal mol}^{-1}$ ),<sup>17,18</sup>  $\text{Fe}^+-\text{O}$  ( $D = 81.4 \pm 1.4 \text{ kcal mol}^{-1}$ ),<sup>16</sup> and  $\text{Co}^+-\text{O}$  ( $D = 76.6 \pm 1.4 \text{ kcal mol}^{-1}$ )<sup>48</sup> bonds readily cleave during hydrocarbon reactions.

One interesting aspect of the  $\text{MoO}^+$  reactions was to determine if the oxygen is incorporated into the resulting hydrocarbon ligand on  $\text{Mo}^+$ . Jacobson has shown that discrete oxo ligands bound to a metal center can undergo isotopic oxygen exchange with  $^{18}\text{O}_2$ <sup>49</sup> and  $\text{H}_2^{18}\text{O}$ .<sup>50</sup> This should not occur if the oxygen is attached to another ligand on the metal. Therefore, the major product ions formed in the reactions of  $\text{MoO}^+$  with hydrocarbons were subsequently reacted with  $\text{H}_2^{18}\text{O}$ . For most  $\text{MoOC}_m\text{H}_n^+$  studied, traces of  $\text{Mo}^{18}\text{OC}_m\text{H}_n^+$  were produced, reaction 6, indi-



cating that the oxygen was not incorporated into the hydrocarbon ligand. However, this reaction was always in competition with the much more facile process of oxygen abstraction to produce  $\text{MoO}^{18}\text{OC}_m\text{H}_n^+$ .

$\text{MoO}^+$  also readily abstracts oxygen from  $\text{H}_2^{18}\text{O}$  to yield  $\text{MoO}^{18}\text{O}^+$ , reaction 7. Based on the literature values of  $\Delta H_f^\circ(\text{MoO}^+) = 267 \text{ kcal mol}^{-1}$  and  $\Delta H_f^\circ(\text{MoO}_2^+) = 213 \text{ kcal mol}^{-1}$ ,<sup>33</sup> abstraction of oxygen from water would be endo-



thermic by  $4 \text{ kcal mol}^{-1}$ . This is obviously not the case, and although this is not a major deviation, it does suggest that there is some error in the literature values. The observation of reaction 7 indicates that  $D(\text{OMo}^+-\text{O}) > 117 \text{ kcal mol}^{-1}$ .<sup>33</sup> This agrees with the absence of reaction between  $\text{MoO}_2^+$  and  $\text{D}_2$ , which yields  $D(\text{OMo}^+-\text{O}) > 119 \text{ kcal mol}^{-1}$ . Both results suggest that the literature value of  $D(\text{OMo}^+-\text{O}) = 114 \text{ kcal mol}^{-1}$ <sup>33</sup> is low.

Methane does not react with  $\text{MoO}^+$ , suggesting that  $D(\text{MoO}^+-\text{CH}_2) < 111 \text{ kcal mol}^{-1}$ .<sup>33</sup> Ethane reacts with  $\text{MoO}^+$  via primarily the elimination of  $\text{H}_2$ , reaction 8, with a minor amount (5%) of  $2\text{H}_2$  loss, reaction 9. The amount



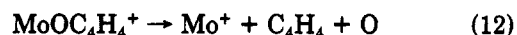
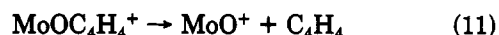
of  $2\text{H}_2$  loss increases to 20–30% if the reactant ions are not subjected to collisional cooling with xenon prior to the reaction. This is the only instance in which collisional

cooling has a significant effect on the product ion distributions. This suggests that only a small amount of energy is required to dehydrogenate  $\text{MoOC}_2\text{H}_4^+$ . CID confirms this, with the elimination of  $\text{H}_2$  from  $\text{MoOC}_2\text{H}_4^+$  occurring in high abundance at low collision energies. At progressively higher energies, both  $\text{MoOC}_2\text{H}_2^+$  and  $\text{MoOC}_2\text{H}_4^+$  dissociate to form  $\text{MoO}^+$  and  $\text{Mo}^+$ . These primary product ions also singly dehydrogenate ethane.

The reaction of ethane and  $\text{MoO}^+$  can be envisioned as proceeding via metal insertion into a C–H bond followed by the reductive elimination of  $\text{H}_2$ . In this process, which is shown in Scheme II, the oxo ligand does not actively participate in the reaction.<sup>51</sup> The absence of  $\text{H}_2\text{O}$  elimination indicates that the combination of H and O to form  $\text{H}_2\text{O}$  at the metal center is slow relative to  $\text{H}_2$  formation. In fact, due to the strong  $\text{Mo}^+-\text{O}$  bond, the production of  $\text{H}_2\text{O}$  from the reactions of  $\text{MoO}^+$  and small hydrocarbons is probably endothermic. If this process is endothermic, then  $D(\text{Mo}^+-\text{C}_2\text{H}_4) < 29 \text{ kcal mol}^{-1}$ , which is consistent with the findings of the  $\text{Mo}^+$  and ethane data which suggest that  $D(\text{Mo}^+-\text{C}_2\text{H}_4) \leq 33 \text{ kcal mol}^{-1}$ .<sup>33</sup>

The production of  $\text{Mo}^+$  and ethanol from  $\text{MoO}^+$  and ethane is not observed. This process would be interesting, given the hydrocarbon oxidation capabilities of molybdenum compounds in solution.<sup>1–7</sup> Unfortunately, the process should be approximately  $18 \text{ kcal mol}^{-1}$  endothermic<sup>33</sup> and therefore should not occur in the FTMS.

Double dehydrogenation dominates in the reactions of  $\text{MoO}^+$  with propane and butane. Both reactions occur readily, with the efficiency increasing toward unity as the number of carbons in the linear alkane increases. As the data in Table V indicate, the secondary reactions with propane involve C–C bond cleavage. A tendency toward C–C bond cleavage is also observed in the CID processes. For example,  $\text{MoOC}_4\text{H}_4^+$  produced from the reaction of  $\text{MoO}^+$  and butane dissociates to yield  $\text{MoOC}_3\text{H}_2^+$  at low energies and  $\text{MoO}^+$  and  $\text{Mo}^+$  at higher energies (reactions 10–12). All  $\text{MoOC}_m\text{H}_n^+$  that were studied by CID gave



abundant  $\text{MoO}^+$  upon collisional activation. This, along with the  $\text{H}_2^{18}\text{O}$  oxygen-exchange data, strongly suggests that no oxygen incorporation into the hydrocarbon ligands on  $\text{Mo}^+$  is occurring.

The 2-methylpropane and  $\text{MoO}^+$  reaction is unique, with the dominant process being C–C bond cleavage and the elimination of  $\text{CH}_4$  and  $\text{H}_2$  to produce  $\text{MoOC}_3\text{H}_4^+$ , reaction 13. Double and single dehydrogenation is also observed, reactions 14 and 15. This contrasts the  $\text{Mo}^+$  reaction

(51) In Schemes II and III, attachment of oxygen to  $\text{Mo}^+$  has been represented by a single bond. However, the exact nature of this bonding (i.e., single or double bonds) is unknown.

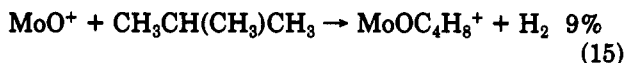
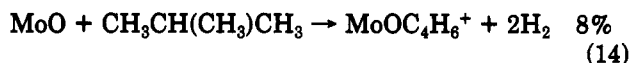
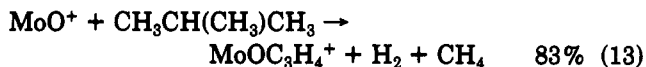
(46) Aristov, N.; Armentrout, P. B. *J. Am. Chem. Soc.* 1984, 106, 4065.

(47) Fisher, E. R.; Elkind, J. L.; Clemmer, D. E.; Georgiadis, R.; Loh, S. K.; Aristov, N.; Sunderlin, L. S.; Armentrout, P. B. *J. Chem. Phys.* 1990, 93, 2676.

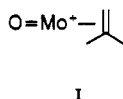
(48) Cassidy, C. J.; McElvany, S. W. Unpublished results.

(49) Klaassen, J. J.; Jacobson, D. B. *J. Am. Chem. Soc.* 1988, 110, 974.

(50) Jacobson, D. B. *Inorg. Chem.* 1989, 28, 2022.



which involves exclusive  $\text{H}_2$  loss. The fact that  $\text{CH}_4$  loss is only found in conjunction with dehydrogenation, and not alone, suggests that  $\text{MoO}^+$  does not initially insert into a C–C bond. Instead, initial insertion of  $\text{MoO}^+$  into the central C–H bond (which is the weaker of the two types of C–H bonds in 2-methylpropane<sup>52</sup>), followed by a  $\beta$ -hydride shift and the reductive elimination of  $\text{H}_2$ , would result in a  $\text{MoO}^+$ -2-methylpropene species, structure I.



This activated intermediate may then eliminate  $\text{CH}_4$  (reaction 13) or  $\text{H}_2$  (reaction 15). This mechanism is supported by the fact that  $\text{CH}_4$  elimination and  $\text{H}_2$  elimination are major processes in the reaction of  $\text{MoO}^+$  with 2-methylpropene.

Carbon-carbon bond cleavage continues in the secondary reactions of  $\text{MoOC}_m\text{H}_n^+$  with 2-methylpropane. In addition, the major process (60%) in the reaction of  $\text{MoOC}_4\text{H}_8^+$  with 2-methylpropane is  $\text{H}_2\text{O}$  elimination. For the  $\text{MoOC}_m\text{H}_n^+$  and alkane reactions studied, this is the only instance in which  $\text{H}_2\text{O}$  loss was observed.

**Reactions of  $\text{MoO}^+$  with Small Alkenes.** The reactions of  $\text{MoO}^+$  and alkenes are efficient, with essentially every collision resulting in product formation. With the exception of the 2-methylpropene reaction, dehydrogenation again dominates. CID of the product ions and oxygen-exchange reactions with  $\text{H}_2^{18}\text{O}$  provides no evidence to suggest that oxygen is being incorporated into the resulting hydrocarbon ligand. These results sharply contrast the reactions of the first-row group 6 ion  $\text{Cr}^+$ . Kang and Beauchamp found that  $\text{CrO}^+$  reacts with small alkenes via primarily C–C bond cleavage with the elimination of hydrocarbons and by transfer of oxygen to the alkene to yield loss of an oxygenated hydrocarbon.<sup>17</sup> While the production of  $\text{M}^+$  via epoxide elimination is slightly exothermic for  $\text{Cr}^+$ , this process is endothermic by approximately 30 kcal mol<sup>-1</sup> for  $\text{Mo}^+$ <sup>33</sup> and is therefore not observed in the present study.

The  $\text{MoO}^+$  ions sequentially dehydrogenate five ethene molecules, producing  $\text{MoOC}_m\text{H}_n^+$ ,  $m = 2, 4, 6, 8$ , and 10. Reactions with the first three molecules of ethene proceed rapidly at near the collision rate; however,  $\text{MoOC}_8\text{H}_8^+$  production from  $\text{MoOC}_6\text{H}_6^+$  is very slow. When collisionally activated,  $\text{MoOC}_6\text{H}_6^+$  eliminates predominantly  $\text{C}_2\text{H}_6$  at low energies, with  $\text{Mo}^+$  forming at higher energies. Therefore, the reactivity and CID data are again consistent with a stable  $\text{OMo}^+$ -benzene structure. For  $\text{MoOC}_m\text{H}_n^+$ ,  $m = 2, 4$ , and 8, the dominant low-energy CID process is  $\text{C}_2\text{H}_2$  elimination, with  $\text{MoO}^+$  and  $\text{Mo}^+$  forming at higher energies. The elimination of  $\text{H}_2$  is also observed as a minor low-energy pathway. These CID data suggest that the oxygen is not incorporated into the hydrocarbon ligand(s), but the number of hydrocarbon ligands on  $\text{Mo}^+$  is not established.

Dehydrogenation is again the major process in the  $\text{MoO}^+$  reaction with propene, but methane elimination is a minor pathway. The reactions of  $\text{MoOC}_3\text{H}_4^+$ , the major primary product, indicate that C–C cleavage is dominant in the secondary reactions. In addition to the major products given in Table V, a variety of minor products involving C–C bond cleavage are generated. CID of the major product ions,  $\text{MoOC}_3\text{H}_4^+$  and  $\text{MoC}_4\text{H}_8^+$ , results in  $\text{H}_2$  elimination at low energies and  $\text{MoO}^+$  and  $\text{Mo}^+$  formation at higher energies. Minor amounts of C–C bond cleavage also occur upon collisional activation. These results are consistent with intact  $\text{C}_m\text{H}_n$  ligands attached to  $\text{MoO}^+$ .

The reactions of 1-butene and *cis*-2-butene with  $\text{MoO}^+$  proceed primarily by elimination of two molecules of  $\text{H}_2$ . This is interesting because  $\text{Mo}^+$  reductively eliminates only a single  $\text{H}_2$  in its reactions with butene isomers. In the secondary reactions of  $\text{MoOC}_m\text{H}_n^+$  with butenes, selective bond cleavage no longer exists, with C–H and C–C cleavage processes occurring in abundance. These reactions were not studied in detail due to the large number of pathways. While the subsequent reactions produced some loss of the oxygen atom, this was minor compared to  $\text{H}_2$  and hydrocarbon elimination.

The reaction of 2-methylpropene with  $\text{MoO}^+$  is unique because  $\text{H}_2\text{O}$  loss occurs as a primary pathway. However, this process is minor (5%) and the elimination of  $\text{CH}_4$ ,  $\text{H}_2$ , and  $2\text{H}_2$  dominate. These four primary ions continue to react with 2-methylpropene, each producing multiple products involving the elimination of  $\text{H}_2\text{O}$ ,  $\text{H}_2$ , and small hydrocarbon molecules. All selective bond cleavage characteristics of  $\text{MoO}^+$  are lost as hydrocarbon ligands become attached to the metal oxide ion. CID on the major product ions continues to yield facile  $\text{MoO}^+$  formation, which suggests that the oxygen atom is not incorporated into the hydrocarbon chains.

**Reactions of  $\text{MoO}^+$  with Selected  $\text{C}_6$  Hydrocarbons.**  $\text{MoO}^+$  reacts with both cyclohexane and cyclohexene to produce only  $\text{MoOC}_6\text{H}_6^+$ . The reaction efficiencies are near unity, indicating that almost every collision of  $\text{MoO}^+$  and the neutral results in the formation of  $\text{MoOC}_6\text{H}_6^+$ . Under CID conditions,  $\text{MoOC}_6\text{H}_6^+$  produces primarily  $\text{MoO}^+$ , with traces of  $\text{MoOC}_6\text{H}_4^+$  forming at low energies. This suggests a  $\text{OMo}^+$ -benzene structure, with no oxygen incorporation into the benzene ring.  $\text{MoOC}_6\text{H}_6^+$  does not react further with either precursor neutral.

$\text{MoO}^+$  reacts at near the collision rate with *n*-hexane. Multiple dehydrogenation is a major process, but C–C bond cleavage involving  $\text{C}_2\text{H}_6$  and  $\text{H}_2$  elimination also occurs. As was the case with 2-methylpropane, the presence of  $\text{C}_2\text{H}_6$  loss only in conjunction with  $\text{H}_2$  loss suggests that  $\text{MoO}^+$  is not inserting into a C–C bond but instead  $\text{C}_2\text{H}_6$  is eliminated from an activated intermediate following initial  $\text{H}_2$  loss. No secondary reactions were observed. This is consistent with the lack of secondary reactions for the  $\text{MoO}^+$ /*n*-butane system and suggests that the tendency toward secondary reactions decreases as the length of the alkane chain increases. This is probably the result of steric factors at the metal center. A similar trend has been noted in the reactions of  $\text{VO}^+$ .<sup>19</sup>

**Reactions of  $\text{MoO}_2^+$  with Small Alkanes.** Two structural possibilities exist for  $\text{MoO}_2^+$ : an oxygen molecule bound to  $\text{Mo}^+$ ,  $\text{Mo}^+-\text{O}_2$ ,<sup>53</sup> or two oxo ligands attached to  $\text{Mo}^+$ ,  $\text{O}-\text{Mo}^+-\text{O}$ . These structures are expected to exhibit very different gas-phase reactivities. Therefore,

(53) Dioxygen ligands are known to exist in solution. For examples, see: (a) Taube, H. *Prog. Inorg. Chem.* 1986, 34, 607. (b) Dengel, A. C.; Griffith, W. P.; Powell, R. D.; Skapski, A. C. *J. Chem. Soc., Chem. Commun.* 1986, 7, 555.



Table VI. Secondary Reactions of  $\text{MoO}_2\text{C}_m\text{H}_n^+$  with Hydrocarbons

hydrocarbon	reactant ion	products	rel abundance, %
ethene	$\text{MoO}(\text{CO})^+$	$\text{MoOC}_2\text{H}_4^+ + \text{CO}$	100
propene	$\text{MoO}_2\text{CH}_4^+$	$\text{MoO}_2\text{C}_2\text{H}_6^+ + \text{C}_2\text{H}_4$	25
		$\text{MoO}_2\text{C}_3\text{H}_8^+ + \text{CH}_4$	35
		$\text{MoO}_2\text{C}_4\text{H}_{10}^+ + \text{H}_2$	40
	$\text{MoO}_2\text{C}_2\text{H}_6^+$	$\text{MoOC}_2\text{H}_6^+ + \text{H}_2\text{O}$	100
1-butene	<i>a</i>		
<i>cis</i> -2-butene	<i>a</i>		
2-methylpropene	<i>a</i>		

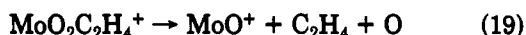
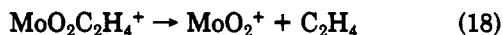
<sup>a</sup>The primary products from the reactions of  $\text{MoO}_2^+$  with the three butene isomers were very reactive with the neutral. Due to the extreme complexity of the spectra, the isolation of reaction pathways was not performed.

isotopic oxygen-exchange reactions and CID experiments were conducted to determine the  $\text{MoO}_2^+$  structure. Reaction with  $\text{H}_2^{18}\text{O}$  gave two sequential isotopic oxygen exchanges, with all  $\text{MoO}_2^+$  reacting.  $\text{MoO}_2^+$  dissociates to yield  $\text{MoO}^+$  at low energies and  $\text{Mo}^+$  at higher energies. These data indicate that the ions involved in this study contain two oxo ligands,  $\text{O}-\text{Mo}^+-\text{O}$ .

While the primary reactions of  $\text{Mo}^+$  and  $\text{MoO}^+$  with alkanes were limited to dehydrogenation,  $\text{MoO}_2^+$  readily eliminates both  $\text{H}_2\text{O}$  and hydrocarbons. In addition,  $\text{MoO}_2^+$  is slightly slower to react than  $\text{MoO}^+$  (possibly due to steric factors) but reacts considerably faster than  $\text{Mo}^+$ . The  $\text{OMo}^+-\text{O}$  bond is reported to have a dissociation energy of  $114 \text{ kcal mol}^{-1}$ , which makes it roughly equal in strength to the  $\text{Mo}^+-\text{O}$  bond.<sup>33</sup> This means that oxygen transfer to produce alcohols from hydrocarbons is still endothermic by approximately  $20 \text{ kcal mol}^{-1}$ <sup>33</sup> and is not observed.

Isotopic oxygen-exchange reactions were employed on the major  $\text{MoO}_2\text{C}_m\text{H}_n^+$  products formed from the reactions of  $\text{MoO}_2^+$  with small hydrocarbons. In all cases, two sequential  $^{18}\text{O}/^{16}\text{O}$  exchanges were observed. In addition,  $\text{MoO}_2^+$  is a dominant product in the CID of these species. This indicates that the  $\text{MoO}_2\text{C}_m\text{H}_n^+$  product ions have two discrete oxo ligands bound to  $\text{Mo}^+$ . Again, no evidence is found for oxygen incorporation into the hydrocarbon ligands.

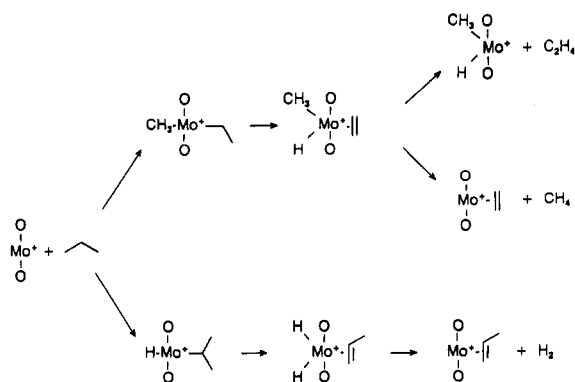
Ethane reacts with  $\text{MoO}_2^+$  by single dehydrogenation to produce  $\text{MoO}_2\text{C}_2\text{H}_4^+$ , which does not react further. (In fact, as the lack of data in Table VI indicates, no secondary reactions were observed for any of the alkanes studied.) This ion dissociates by reactions 16–19 when collisionally activated. Dehydration (reaction 16) occurred in high



abundance at low-energy conditions. This again contrasts the behavior of  $\text{MoOC}_m\text{H}_n^+$ , which eliminated  $\text{H}_2$  at low energies. Coordinative saturation may also be playing a role in the CID processes, with the decreased number of sites available on molybdenum facilitating transfer of hydrogen atoms to an oxygen atom rather than bonding to the metal. Reactions 17–19 occur at progressively higher energies. The formation of  $\text{MoO}_2\text{H}_2^+$  is interesting and may involve a metal hydroxide,  $\text{Mo}(\text{OH})_2^+$ .

The reactions of  $\text{MoO}_2^+$  with propane dramatically differ from the  $\text{MoO}^+$  reactions. As the data in Table I indicate,  $\text{MoO}_2^+$  dehydrogenates propane to a lesser extent than

Scheme III

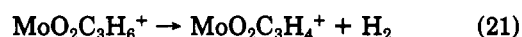


does  $\text{MoO}^+$ . This is opposite of the findings of the ethane reactions. Also interesting is the extensive C–C bond cleavage (elimination of  $\text{C}_2\text{H}_4$  and  $\text{CH}_4$ ) seen in the  $\text{MoO}_2^+$  reaction. These processes do not involve  $\text{H}_2$  elimination. This suggests that  $\text{MoO}_2^+$  is capable of undergoing exothermic processes involving insertion into the C–C bonds of hydrocarbons. A mechanism for  $\text{MoO}_2^+$  insertion into the C–C bond of propane, followed by a  $\beta$ -hydride shift and the reductive elimination of hydrocarbon molecules is shown in Scheme III.<sup>51</sup> CID of the product ions yields  $\text{MoO}_2^+$  as a major low-energy process. (In addition,  $\text{MoO}_2\text{C}_2\text{H}_4^+$  from propane also eliminates  $\text{H}_2\text{O}$  in a manner identical to the ions produced from ethane.) These ions undergo two sequential isotopic oxygen exchanges. Thus, there is no evidence to show that the oxygen atoms are playing active roles in the reactions.

The nature of the  $\text{Mo}^+-\text{O}$  bonding at each step in Scheme III (and also in Scheme II) is unknown. In solution, oxomolybdenum groups are generally considered to involve double bonds.<sup>1</sup> However, if the oxo ligands are only spectators in the gas-phase reactions (as our data suggest), then some steps in the  $\text{MoO}_2^+$  reactions must involve molybdenum-to-oxygen bonds with single-bond character. This is because  $\text{Mo}^+$  is a  $d^5$  system allowing only five covalent bonds to the metal. Therefore, as the number of oxygens attached to  $\text{Mo}^+$  increases, coordinative saturation becomes more important in the reactions. This effect undoubtedly contributes to the differences in product ion formation and reaction rates seen for  $\text{MoO}_2^+$ ,  $\text{MoO}^+$ , and  $\text{Mo}^+$ . Also notable is the complete lack of secondary reactions found between  $\text{MoO}_2\text{C}_m\text{H}_n^+$  and alkanes, suggesting that coordinative saturation is hindering further reactions.

As shown in Scheme III,  $\text{MoO}_2^+$  cleaves both C–C and C–H bonds. For propane, the C–C bond cleavage product,  $\text{MoO}_2\text{C}_2\text{H}_4^+$ , is unusual and its structure is unclear. This ion also forms in the propene reactions via the elimination of acetylene. In both instances, low-energy CID yields abundant  $\text{CH}_3$  and  $\text{CH}_4$  losses, suggesting that a methyl ligand is bound to  $\text{Mo}^+$ . The remaining H may reside on  $\text{Mo}^+$  or on oxygen (as a hydroxyl ligand) or in equilibrium between the two positions.

The dehydrogenation product from propane,  $\text{MoO}_2\text{C}_3\text{H}_6^+$ , undergoes two major low-energy CID processes,  $\text{H}_2\text{O}$  loss (reaction 20) and  $\text{H}_2$  loss (reaction 21).



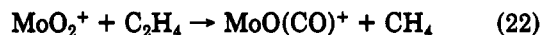
The elimination of  $\text{H}_2$ , reaction 21, is interesting because double dehydrogenation of propane did not occur as a primary reaction process. The loss of  $\text{H}_2\text{O}$  continues the trend observed for ethane regarding facile dehydrogenation

of  $\text{MoO}_2\text{-(alkene)}^+$  species. At progressively higher energies,  $\text{MoO}_2\text{H}^+$ ,  $\text{MoO}_2^+$ ,  $\text{MoO}^+$ , and  $\text{Mo}^+$  are produced.

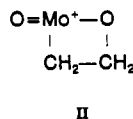
The insertion of  $\text{MoO}_2^+$  into C-C bonds continues with *n*-butane and 2-methylpropane. Again, dehydrogenation is not as extensive as it was in the  $\text{MoO}^+$  reactions. Instead, loss of  $\text{H}_2\text{O}$  and  $\text{H}_2$  is a major process in the reactions with  $\text{MoO}_2^+$ . This suggests that as the number and size of ligands bound to  $\text{Mo}^+$  increases, the attachment of O and H on the metal center to produce  $\text{H}_2\text{O}$  becomes more favorable.

**Reactions of  $\text{MoO}_2^+$  with Small Alkenes.** The reactions with small alkenes demonstrate that the addition of an oxygen atom to  $\text{MoO}^+$  dramatically affects reactivity. Dehydrogenation and C-C bond cleavage followed by the elimination of small hydrocarbons are prevalent. The product ion distributions shown in Table III indicate that the selective C-H bond cleavage exhibited by  $\text{Mo}^+$  and  $\text{MoO}^+$  is totally absent, with  $\text{MoO}_2^+$  readily breaking C-H, C-C, and Mo-O bonds.

The reactions of  $\text{MoO}_2^+$  with ethene are unique because the major process is hydrocarbon oxidation to produce  $\text{MoO}(\text{CO})^+$ , reaction 22. This is the only instance of



oxygen transfer found in the reactions of  $\text{MoO}_y^+$ ,  $y = 1$  and 2, with small hydrocarbons. The rapid displacement of CO by ethene, to yield  $\text{MoOC}_2\text{H}_4^+$ , indicates that an intact CO ligand is bound to  $\text{MoO}^+$  and that  $D(\text{OMo}^+-\text{C}_2\text{H}_4) > D(\text{OMo}^+-\text{CO})$ . Since  $\text{MoO}(\text{CO})^+$  and  $\text{MoO}(\text{C}_2\text{H}_4)^+$  have the same nominal mass ( $m/z$  136), high-resolution and exact mass measurements were used to confirm the presence of the two ions. As Figure 1 indicates, isolation of  $\text{MoO}(\text{CO})^+$  by the selected wave form inverse Fourier transform (SWIFT) technique,<sup>54</sup> followed by a variable delay to allow time for reaction, demonstrates the presence of the secondary reaction. The mechanism for  $\text{MoO}(\text{CO})^+$  formation is not established. One possibility involves decomposition of a metallacycle intermediate II that is



produced from a four-center cycloaddition process. Similar intermediates have been proposed in the reactions of  $\text{CrO}^+$ <sup>17</sup> and  $\text{OsO}_y$ ,  $y = 1-4$ ,<sup>20</sup> with various small molecules. While these metal oxide ions do not oxidize ethene to produce CO,  $\text{CoO}^+$ <sup>48</sup> undergoes an analogous process to yield  $\text{CoCO}^+$  and  $\text{CH}_4$ .

The three major reaction pathways of  $\text{MoO}_2^+$ —hydrocarbon elimination, dehydration, and dehydrogenation—are all demonstrated in the propene reactions. The product following acetylene elimination,  $\text{MoO}_2\text{CH}_4^+$ , dissociates under low-energy CID conditions to eliminate  $\text{CH}_4$  as the major product. This indicates that  $\text{CH}_4$  is more weakly bound than O.  $\text{MoOC}_3\text{H}_4^+$  readily fragments via  $\text{H}_2$  elimination, which is analogous to the dissociation of  $\text{MoOC}_m\text{H}_n^+$  produced from the  $\text{MoO}^+$  reactions.  $\text{MoO}_2\text{C}_3\text{H}_4^+$  loses  $\text{H}_2\text{O}$  readily upon collisional activation, although minor amounts of hydrocarbon elimination also occur. The highest energy CID processes for all three primary products involve  $\text{MoO}_y^+$  formation, again suggesting that the oxygens are not attached to hydrocarbon species on the metal.

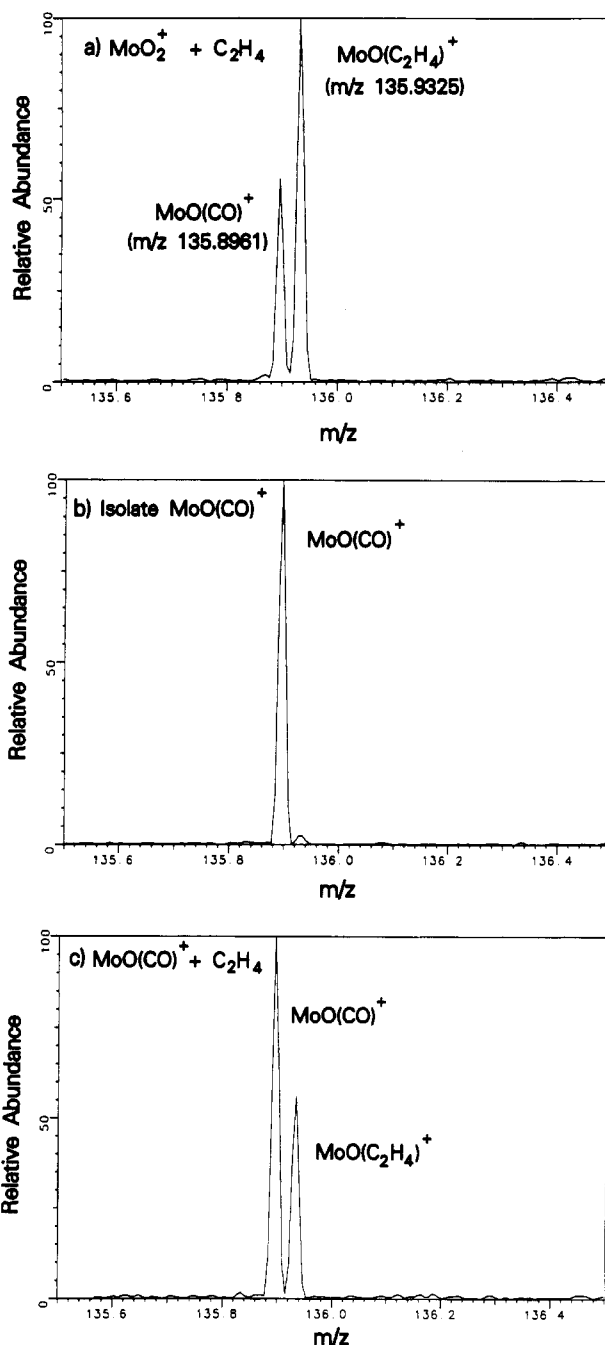


**Figure 1.** (a) Portion of the mass spectrum near  $m/z$  136 following a 2-s reaction of  $^{92}\text{MoO}_2^+$  ( $m/z$  124) with  $\text{C}_2\text{H}_4$  at  $2 \times 10^{-8}$  Torr. Note the presence of two product ions at nominal  $m/z$  136 corresponding to  $\text{MoO}(\text{CO})^+$  and  $\text{MoO}(\text{C}_2\text{H}_4)^+$ . (b) Mass selection of  $\text{MoO}(\text{CO})^+$  from (a) using the SWIFT technique. (c) Mass spectrum following a 0.5-s reaction of  $\text{MoO}(\text{CO})^+$  (b) with  $\text{C}_2\text{H}_4$ . Note the displacement of CO by  $\text{C}_2\text{H}_4$ .

Ethene elimination is the major process in the reactions of  $\text{MoO}_2^+$  with 1-butene, *cis*-2-butene, and 2-methylpropene. However, dehydration, dehydrogenation, and the elimination of other hydrocarbons also occur readily. These reactions proceed near the collision rate, and the primary product ions each undergo additional reactions with the neutral butene. The resulting spectra are very complex, containing 30 or more product ions; therefore, these reaction pathways were not studied in detail. The secondary reactions also exhibited no bond selectivity, with all three major reaction pathways occurring in abundance. These reactions terminate with the production of  $\text{MoC}_{12}\text{H}_n^+$  and  $\text{MoOC}_{12}\text{H}_n^+$  species. A notable feature of these reactions is that one or both oxygens are eliminated,

(54) Marshall, A. G.; Wang, T. C. L.; Chen, L.; Ricca, T. L. In *Fourier Transform Mass Spectrometry: Evolution, Innovation, and Applications*; Buchanan, M. V., Ed.; ACS Symposium Series 359; American Chemical Society: Washington, DC, 1987; pp 21-33.

freeing up coordination sites on  $\text{Mo}^+$  and making the metal center available for additional reactions.

**Reactions of  $\text{MoO}_2^+$  with Selected  $\text{C}_6$  Hydrocarbons.**  $\text{MoO}_2^+$  is readily dehydrated in its reactions with cyclohexane and cyclohexene, producing  $\text{MoOC}_6\text{H}_6^+$  as the major product. Cyclohexene also yields  $\text{MoO}_2\text{C}_6\text{H}_6^+$  and  $\text{MoO}_2\text{C}_6\text{H}_5^+$  as minor products.  $\text{MoOC}_6\text{H}_6^+$  undergoes CID in the manner previously discussed for ions generated from  $\text{MoO}^+$ , indicating a  $\text{OMo}^+$ -benzene structure. No secondary reactions occur.

The  $\text{MoO}_2^+$  and *n*-hexane reaction continues to differ from the cyclohexane and cyclohexene reactions. The four pathways observed are completely different from the  $\text{MoO}^+$  pathways, involving more extensive hydrocarbon loss and dehydration than occurs with  $\text{MoO}^+$ . No secondary reactions were observed, aside from minor  $\text{MoOC}_6\text{H}_6^+$  formation. The  $\text{C}_2\text{H}_6$  elimination product,  $\text{MoO}_2\text{C}_4\text{H}_8^+$ , undergoes facile low-energy CID to produce  $\text{MoOC}_4\text{H}_6^+$  (via  $\text{H}_2\text{O}$  loss). This suggests that in the primary reaction  $\text{MoOC}_4\text{H}_6^+$  was produced by sequential  $\text{C}_2\text{H}_6$  and  $\text{H}_2\text{O}$  losses.

### Conclusions

Dehydrogenation is the dominant process in the reactions of  $\text{Mo}^+$ ,  $\text{MoO}^+$ , and  $\text{MoO}_2^+$  with small hydrocarbons. The strong  $\text{Mo}^+-\text{O}$  and  $\text{OMo}^+-\text{O}$  bonds are rarely cleaved in these reactions. Little evidence is found for the production of oxygenated hydrocarbons, either as neutral reaction products or as ligands bound to  $\text{Mo}^+$ . The only exception is the reaction of  $\text{MoO}_2^+$  with ethene, which produces an intact CO on the metal,  $\text{MoO}(\text{CO})^+$ .

While hydrocarbon oxidation is rare, the attachment of oxygen atoms to  $\text{Mo}^+$  does affect the chemistry. The addition of ligands leads to increased reaction rates relative to the slow rates of reaction of the  $d^5$  system  $\text{Mo}^+$ , with several  $\text{MoO}^+$  and  $\text{MoO}_2^+$  reactions proceeding at or near

the collision rate. Secondary  $\text{MoC}_m\text{H}_n^+$  reactions also proceed rapidly, indicating that this effect is not unique to oxygen. In addition, variations are seen in product ion distributions between the three ions, and for  $\text{MoO}_2^+$ , unique reaction pathways involving dehydration and the elimination of small hydrocarbons occur. The elimination of small hydrocarbons in the  $\text{MoO}_2^+$  reactions is particularly interesting because it suggests that  $\text{MoO}_2^+$  is capable of inserting into the C-C bonds of organic molecules, while  $\text{Mo}^+$  and  $\text{MoO}^+$  almost exclusively yield products that result from C-H insertion.

The extent of reactivity also differs among the  $\text{MoO}_y^+$  species. The  $\text{Mo}^+$  ion undergoes multiple reactions with hydrocarbons, producing  $\text{MoC}_m\text{H}_n^+$  species containing up to 12 carbon atoms. With the exception of  $\text{MoC}_{12}\text{H}_{12}^+$ , which has a dibenzene structure, these hydrocarbon species may exist as one intact ligand on  $\text{Mo}^+$ , indicating that  $\text{Mo}^+$  is capable of extensive ligand coupling. The  $\text{MoO}^+$  reactions terminate with smaller  $\text{MoOC}_m\text{H}_n^+$  products which usually contain only eight carbon atoms. In contrast,  $\text{MoO}_2^+$  reactions end with primary product formation unless the secondary reactions involve elimination of oxygen. Therefore, a major factor in reactivity differences between  $\text{Mo}^+$ ,  $\text{MoO}^+$ , and  $\text{MoO}_2^+$  is the number of available coordination sites on molybdenum.

**Acknowledgment.** We thank the Office of Naval Research for funding of this work, and C.J.C. thanks the Naval Research Laboratory for funding as a National Research Council postdoctoral research associate.

**Registry No.**  $\text{Mo}^+$ , 16727-12-1;  $\text{MoO}^+$ , 71252-77-2;  $\text{MoO}_2^+$ , 16984-32-0;  $\text{C}_2\text{H}_6$ , 74-84-0;  $\text{CH}_3\text{CH}(\text{CH}_3)\text{CH}_3$ , 75-28-5;  $\text{C}_2\text{H}_4$ , 74-85-1; propane, 74-98-6; butane, 106-97-8; propene, 115-07-1; 1-butene, 106-98-9; *cis*-2-butene, 590-18-1; 2-methylpropene, 115-11-7; cyclohexane, 110-82-7; cyclohexene, 110-83-8; *n*-hexane, 110-54-3.

OM9106701